ENERGY EFFICIENCY IN WIRELESS NETWORKS

A Dissertation

by

EUN-SUN JUNG

Submitted to the Office of Graduate Studies of
Texas A&M University
in partial fulfillment of the requirements for the degree of

DOCTOR OF PHILOSOPHY

August 2005

Major Subject: Computer Science

ENERGY EFFICIENCY IN WIRELESS NETWORKS

A Dissertation

by

EUN-SUN JUNG

Submitted to the Office of Graduate Studies of
Texas A&M University
in partial fulfillment of the requirements for the degree of

DOCTOR OF PHILOSOPHY

Approved by:

Chair of Committee,	Nitin H. Vaidya
Committee Members,	Riccardo Bettati
	Narasimha Reddy
	Jennifer Welch
Head of Department,	Valerie E. Taylor

August 2005

Major Subject: Computer Science

ABSTRACT

Energy Efficiency in Wireless Networks. (August 2005)

Eun-Sun Jung, B.S., Dankook University;

M.S., University of London

Chair of Advisory Committee: Dr. Nitin H. Vaidya

Energy is a critical resource in the design of wireless networks since wireless devices are usually powered by batteries. Battery capacity is finite and the progress of battery technology is very slow, with capacity expected to make little improvement in the near future. Under these conditions, many techniques for conserving power have been proposed to increase battery life.

In this dissertation we consider two approaches to conserving the energy consumed by a wireless network interface. One technique is to use power saving mode, which allows a node to power off its wireless network interface (or enter a doze state) to reduce energy consumption. The other is to use a technique that suitably varies transmission power to reduce energy consumption. These two techniques are closely related to the MAC (Medium Access Control) layer.

With respect to power saving mode, we study IEEE 802.11 PSM (Power Saving Mechanism) and propose a scheme that improves its energy efficiency. We also investigate the interaction between power saving mode and TCP (Transport Control Protocol). As a second approach to conserving energy, we investigate a simple power control protocol, called BASIC, which uses the maximum transmission power for RTS-CTS and the minimum necessary power for DATA-ACK. We identify the deficiency of BASIC, which increases collisions and degrades network throughput, and propose a power control protocol that addresses these problems and achieves energy savings. Since energy conservation is not an

issue limited to one layer of the protocol stack, we study a cross layer design that combines power control at the MAC layer and power aware routing at the network layer. One power-aware routing metric is minimizing the aggregate transmission power on a path from source to destination. This metric has been used along with BASIC-like power control under the assumption that it can save energy, which we show to be false. Also, we show that the power aware routing metric leads to a lower throughput. We show that using the shortest number of hops in conjunction with BASIC-like power control conserves more energy than power aware routing with BASIC-like power control.

To my parents

ACKNOWLEDGMENTS

First of all, I wish to express my deepest gratitude to my advisor, Dr. Nitin H. Vaidya, for his continual encouragement, help, and guidance throughout my work. This dissertation would not have been possible without his support.

I would also like to extend my sincere thanks to the members of my dissertation committee, Dr. Riccardo Bettati, Dr. Jennifer Welch, and Dr. A. L. Narasimha Reddy, for spending their invaluable time reviewing my dissertation and for suggesting improvements. I am especially grateful to Dr. Bettati and Dr. Welch for their help and care while my advisor was away.

Finally, I would like to thank my parents for their unconditional love, support, and encouragement throughout my studies. This dissertation is dedicated to them.

TABLE OF CONTENTS

CHAPTER Page

I INTRODUCTION 1
A. Motivation 1
B. Dissertation Organization 4

II POWER SAVING MECHANISM 6
A. Power Saving Mechanism for DCF in IEEE 802.11 7
B. Related Work 9
C. Proposed IPSM Scheme 12
1. IPSM Protocol 14
2. Hidden and Exposed Terminal Problems 18
3. Power Saving Mode with TCP 19
D. Performance Evaluation 21
1. Simulation Model 22
a. Wireless LAN 23
b. Random Topology 24
2. Simulation Results 24
a. Wireless LAN: Fixed Network Load 25
b. Wireless LAN: Dynamic Network Load 33
c. Random Topology: CBR Traffic 38
d. Random Topology: TCP Traffic 38
E. Summary 43

III POWER CONTROL 45
A. Related Work 46
B. IEEE 802.11 MAC Protocol 48
C. BASIC Power Control Protocol 52
1. Protocol Description 53
2. Deficiency of the BASIC Protocol 56
D. Proposed Power Control MAC Protocol 59
E. Performance Evaluation 61
1. Simulation Model 62
2. Simulation Topology 62
3. Simulation Results 64
a. Chain Topology: Varying Node Distance 64

CHAPTER Page

b. Chain Topology: Varying Network Load 67
c. Random Topology: Varying Network Load (one hop flow) 70
d. Random Topology: 50 Different Topologies (one hop flow) 70
e. Random Topology: Varying Packet Size (one hop flow) 73
f. Random Topology: 50 Different Topologies (multi-hop flow) 73
F. Summary 76

IV POWER AWARE ROUTING USING POWER CONTROL IN AD HOC NETWORKS 78

A. Related Work 78
B. Power Aware Routing Using Power Control 80
1. An Overview of Power Aware Routing Optimization . . . 80
2. Energy Efficiency of PARO 81
3. Overhearing Process with Power Control 85
C. Performance Evaluation 86
1. Simulation Model 87
2. Simulation Results 88
a. Random Topology: 30 Nodes in 100 x 100 m^2 88
b. Random Topology: 50 Nodes in 1000 x 1000 m^2 . . . 90
c. More Simulation Results in 1000 x 1000 m^2 93
d. TCP Simulation Results in 1000 x 1000 m^2 98
D. Summary 101

V CONCLUSION 103

A. Contributions 103
B. Future Research 104

REFERENCES 105

VITA 114

LIST OF TABLES

TABLE Page

I Number of Flows at Various Power Levels for the Random Topology . . . 64

II BASIC – The Number of Nodes in the Carrier Sensing Zone 66

LIST OF FIGURES

FIGURE		Page
1	Power saving mechanism for DCF: Node A announces a buffered packet for B using an ATIM frame. Node B replies by sending an ATIM-ACK, and both A and B stay awake during the entire beacon interval. The actual data transmission from A to B is completed during the beacon interval. Since C does not have any packet to send or receive, it dozes after the ATIM window.	8
2	IPSM: During the ATIM window node A and B transmit an ATIM and ATIM-ACK, respectively. At the end of the ATIM window, *CIT* is less than *CITThreshold*. Thus, nodes A, B, and C increase their ATIM window size by *ATIMinc*. When the increased ATIM window finishes nodes have *CIT* larger than *CITThreshold*, so A and B start their data transmission. Since C has no packet to send or receive it dozes after the ATIM window. Once completing all the data transmission A and B will also doze for the remaining beacon interval.	16
3	(a) Node A is transmitting a packet to node B; node A is "hidden" for node C. When C starts to transmit a packet to node D, it will cause a collision at B. (b) Node B is transmitting a packet to node A. Since node C is "exposed" to B, node B has to defer its transmission with node D. While the hidden terminal problem results in data loss, the exposed terminal problem simply reduces efficiency.	18
4	In our dynamic network load scenario, the network load changes as the simulation time changes.	24
5	Aggregate throughput: fixed network load.	26
6	Total data delivered per joule: fixed network load.	27
7	Aggregate throughput: fixed data rate (PSMS)	28
8	Total data delivered per joule: fixed data rate (PSMS)	29
9	Aggregate throughput: dynamic network load.	34

FIGURE Page

10 Total data delivered per joule: dynamic network load. 35

11 Aggregate throughput: dynamic rate (PSMS) 36

12 Total data delivered per joule: dynamic rate (PSMS) 37

13 Random topology: 50 nodes with 10 udp flows 39

14 Random topology: 50 nodes with 10 udp flows (PSMS) 40

15 Random topology: 50 nodes with 10 tcp flows 41

16 Random topology: 50 nodes with 10 tcp flows (PSMS) 42

17 Nodes in transmission range can receive and decode packet correctly, whereas nodes in the carrier sensing zone can sense a transmission, but cannot decode it correctly. 50

18 When source and destination nodes transmit RTS and CTS, nodes in transmission range correctly receive these packets and set their NAVs for the duration of the whole packet transmission. However, nodes in the carrier sensing zone only sense the signal and cannot decode it correctly, so these nodes set their NAVs for EIFS duration (when they sense the channel changing state from busy to idle). The purpose of EIFS is to protect an ACK frame at the source node. 51

19 IEEE 802.11 does not prevent collisions completely. After the RTS-CTS handshake, when node C transmits a DATA packet to node D, F cannot sense the DATA transmission since it is in D's carrier sensing zone but not C's. Therefore, when F starts transmitting, it can cause a collision with the reception of the DATA packet at node D. 53

20 Differences in transmission power can lead to increased collisions. 54

21 BASIC scheme: RTS and CTS are transmitted at the highest transmission power level. 54

FIGURE Page

22 BASIC scheme: Suppose node D transmits a packet to node E. Since DATA and ACK are transmitted using the minimum necessary transmission power, nodes in carrier sensing zone (such as A and H) during the RTS-CTS transmission may not sense any signal during DATA-ACK. When these nodes initiate a new transmission by sending RTS at the power level p_{max}, a collision may occur at D and E. The collisions trigger retransmissions, resulting in more energy consumption. . . . 57

23 PCM periodically increases the transmission power during DATA transmission in order to inform nodes in the carrier sensing zone of its transmission. 60

24 Chain topology: 31 nodes with 30 flows. 63

25 Chain topology: Each flow generates traffic at a rate of 1 Mbps: the curves for PCM, PCM40, and 802.11 overlap in (a). 65

26 Chain topology: As the network load increases, aggregate throughput for all four schemes also increases. However, the aggregate throughput of BASIC saturates sooner. 68

27 Chain topology: A large number of retransmissions in BASIC results in more energy consumption. 69

28 Random topology with different network loads: the curves for PCM, PCM40, and 802.11 overlap in (a). 71

29 Random topology with one hop flows for 50 different scenarios using a 1 Mbps data rate per flow. The curves for PCM, PCM40, and 802.11 overlap in (a). 72

30 A random topology with different packet sizes and a 50 Kbps data rate per flow. PCM and PCM40 curves are overlapped in (a). 74

31 Random topology with multi-hop flows for 50 different scenarios using a 1 Mbps data rate per flow. The curves for PCM, PCM40, and 802.11 overlap in (a). 75

32 Chain topology: node A can transmit packets to node C directly, or forward them through an intermediate node B. 81

FIGURE Page

33 Chain topology: the curves for R-PCM and R-802.11 overlap in (a). The aggregate throughput of PARO does not increase beyond 600Kpbs due to the contention between two flows. 83

34 A limitation of a power aware routing protocol with BASIC-like power control: when B is forwarding packets for nodes A and C, D has to defer its transmission, which can cause throughput degradation. 85

35 Random topology with different network loads (30 nodes in 100 x 100m^2): the curves for R-PCM, PARO, and R-802.11 overlap in (a). 89

36 Random topology with different network loads (50 nodes with 10 flows in 1000 x 1000m^2). 91

37 Random topology with different network loads (50 nodes with 20 flows in 1000 x 1000m^2). 92

38 Random topology for 50 different scenarios with a 50 Kbps data rate per flow (50 nodes in 1000 x 1000m^2): 10 flows. 94

39 Random topology for 50 different scenarios with a 50 Kbps data rate per flow (50 nodes in 1000 x 1000m^2): 10 flows – normalized. 95

40 Random topology for 50 different scenarios with a 25 Kbps data rate per flow (50 nodes in 1000 x 1000m^2): 20 flows. 96

41 Random topology for 50 different scenarios with a 25 Kbps data rate per flow (50 nodes in 1000 x 1000m^2): 20 flows – normalized. 97

42 Random topology for 50 different scenarios with TCP traffic (50 nodes in 1000 x 1000m^2): 10 flows. 99

43 Random topology for 50 different scenarios with TCP traffic (50 nodes in 1000 x 1000m^2): 10 flows – normalized. 100

CHAPTER I

INTRODUCTION

A. Motivation

Over the past few decades, a large volume of research has been conducted in the area of wireless networks. Energy is a critical resource in the design of wireless networks, since wireless devices are often powered by batteries. Batteries can provide a finite amount of energy; therefore, to increase battery lifetime, it is important to design techniques to reduce energy consumption by wireless hosts. Many techniques have been proposed to increase battery lifetime. Past research has investigated energy conserving mechanisms at the various layers of the protocol stack, including work on routing [6, 15, 17, 58], medium access control (MAC) [8, 16, 37, 48, 47], and transport protocols [2, 29, 62].

In this dissertation we focus on energy efficiency in a wireless network interface. A wireless network interface can be in an *awake*, *doze*, or *off* state [23]; we may say that a node is in a certain state when its wireless interface is in that state. In the *off* state, the wireless interface consumes no power. In the *doze* state, a node cannot transmit or receive, and consumes very little power. In the *awake* state, a node may be in one of three different modes – transmit, receive, or idle – and consumes somewhat different power in each mode (although all three modes in the awake state consume significantly more power than the doze state). For instance, the Lucent IEEE 802.11 WaveLAN card [35, 49] consumes 1.65 W, 1.4 W, and 1.15 W in the transmit, receive, and idle modes, respectively. In the doze state, the WaveLAN card consumes 0.045 W [35]. More recent data shows that the Cisco AIR-PCM350 card consumes 1.88 W, 1.3 W, 1.08 W in the transmit, receive, and idle modes, respectively, and 0.045 W in the doze state [44]. As we see, the most

---

The journal model is *IEEE Transactions on Automatic Control.*

significant energy consumption in wireless network interface occurs in the transmit mode. Also, a significant amount of energy is consumed even in the idle mode. This occurs due to the CSMA/CA mechanism in IEEE 802.11 which requires each node that is awake to continually listen to the channel.

A wireless network interface consists of several components such as a processor to execute the medium access control (MAC) protocol, a baseband processor, an RF power amplifier, etc. Among these components, an RF power amplifier consumes a significant fraction of energy. As reported in [4], an RF power amplifier may consume more than 50% of the entire power consumption of wireless network interface during transmission. In general, power consumption in a packet transmission varies inversely with distance between two nodes. Consequently, reducing the energy consumption of an RF power amplifier is desirable.

Motivated by these observations, this dissertation considers two approaches to conserving the energy consumed by a wireless network interface. One technique is to use *power saving mode*, which allows a node to power off its wireless network interface (or enter the doze state) to reduce energy consumption in the idle mode [7, 46, 55]. The other is to use a *power control* scheme that suitably varies transmission power to reduce energy consumption in the transmit mode [1, 13, 14, 18, 53, 54].

Power saving mode enables a node to power off its wireless network interface (or to enter the doze state) whenever it does not have a packet to transmit or receive. Although a node in the doze state consumes little energy compared to the transmit or receive modes there exists a wake-up delay for a doze-to-awake transition. For example, 250 μs is reported for the transition in [27]. In this dissertation, we study the power saving mechanism (PSM) in the context of IEEE 802.11, which is the most widely used wireless local area network (WLAN) technology. IEEE 802.11 PSM requires every node to be synchronized by beacon intervals. At the beginning of each beacon interval there exists a time interval, the ATIM

window, where every node has to be awake. During the ATIM window, nodes announce any pending packets to their destinations. Any node that has packets to transmit or receive stays in awake for the remaining beacon interval. On the other hand, nodes that do not have any packet to transmit or receive enter the doze state after the ATIM window to save energy. In IEEE 802.11 PSM, the size of the ATIM window is fixed and identical for every node. However, the optimal ATIM window size depends on network load, the number of nodes in the network, and other factors. If the ATIM window is too small, there is not enough time for all nodes to announce their pending packets. On the other hand, if the size is too large, there is not enough time for actual data transmissions. We propose an adaptive approach, which dynamically adjusts the ATIM window size based on observed network conditions. The proposed solution optimizes IEEE 802.11 PSM in terms of throughput and energy savings. We also investigate the interaction between power saving mode and TCP (Transport Control Protocol).

Power control is a mechanism that allows nodes to vary their transmission power levels. Power control offers two benefits: spatial reuse of the wireless channel, and energy savings. As nodes reduce their transmission power levels the interferences among nodes decreases. This allows simultaneous transmissions in the network, consequently increasing the channel capacity. The other benefit of power control is energy savings. Since nodes utilize only necessary transmission power to transmit a packet they can reduce energy consumption. We investigate a simple power control scheme, called BASIC, for the purpose of energy savings. The BASIC protocol is based on an RTS-CTS handshake in the context of IEEE 802.11. BASIC uses the maximum transmission power for RTS and CTS and the minimum necessary transmission power for DATA and ACK. Although this type of power control protocol does not provide spatial reuse it has been believed that it can conserve energy. However, we identify its shortcoming, which increases collisions and degrades network throughput. We propose a new power control protocol that fixes the problem of

BASIC and achieves energy savings.

The above approaches, power saving mode and power control, are related to the MAC layer. However, energy conservation is not an issue limited to one layer of the protocol stack. Recently, many researchers have focused on cross-layer designs to conserve energy more effectively. One such effort is to employ power control at the MAC layer and to design power aware routing at the network layer. A conventional routing protocol selects a path using the shortest number of hops as a routing metric. It has been proposed that a different routing metric may be useful to achieve energy savings. One such power-aware routing metric is minimizing the aggregate transmission power on a path from source to destination. This metric has been used along with the BASIC-like power control (using the maximum transmission power for RTS-CTS and the minimum necessary transmission power for DATA-ACK) under the assumption that it can save energy, which we show to be false. We show that using the shortest number of hops in conjunction with BASIC-like power control conserves more energy than the power aware routing with BASIC-like power control.

B. Dissertation Organization

The rest of this dissertation is organized as follows. In Chapter II, we first overview IEEE 802.11 power saving mechanism (PSM) that are specified for an IBSS (Independent Basic Service Set) of DCF (Distributed Coordination Function) and survey related work. We then present our proposed scheme, IPSM, and its performance evaluation. In Chapter III, we review the relevant work on power control and provide background information on IEEE 802.11. We describe the BASIC power control protocol and its deficiency, followed by our proposed protocol. Then, we present simulation results. In Chapter IV, we first overview the related work. We then describe a power aware routing protocol with

the BASIC-like power control, PARO, and investigate its energy efficiency. Based on the simulation results we show that using the shortest number of hops with BASIC-like power control can save more energy than PARO. Finally, in Chapter V, we summarize our contributions and conclude the dissertation by discussing future work.

CHAPTER II

POWER SAVING MECHANISM

In this chapter, we study an energy efficient MAC protocol for wireless networks, which attempts to reduce energy consumption by putting the wireless interfaces in a "doze" state when deemed reasonable. Specifically, we consider energy savings in the context of IEEE 802.11 power saving mode.

As mentioned earlier, a wireless network interface can be in *awake* state, *doze* state or *off* state [23]. In this dissertation, we only consider the awake and doze states. Thus, the proposed MAC protocol may place a wireless interface in either the awake or the doze state at any given time. Transition from the doze state to the awake state requires a small duration of time (for instance, the transition time is reported as 250 μs in [27]). Also, transition from the doze state to the awake state results in additional energy consumption during the transition [21].

IEEE 802.11 consists of two components: PCF (Point Coordination Function) and DCF (Distributed Coordination Function). PCF is a centralized medium access control protocol, whereas DCF is a fully distributed protocol [23]. IEEE 802.11 specifies a power saving mechanism for both PCF and DCF. This dissertation focuses on the power saving mechanism (PSM) specified for DCF in an IBSS (Independent Basic Service Set) of IEEE 802.11.

In PSM specified for DCF in an IBSS, time is divided into so-called *beacon intervals* by means of a distributed protocol for beacon transmission. One purpose of the beacons is to synchronize the different nodes [7, 23]. So far as our power saving scheme is concerned, any other mechanism, such as GPS [32], may also be used to synchronize the nodes if available. The beaconing protocol has a shortcoming (particularly when used in conjunction with the power saving mode): that is, when two groups of nodes that are initially

partitioned from each other come together, it may not be possible for them to synchronize their beacon intervals. Some solutions for synchronizing beacon intervals when using DCF in multi-hop wireless networks are proposed in [51]. In this dissertation, we do not consider the problem of synchronizing the nodes, and assume that a mechanism exists for this purpose. For the rest of our discussion, we will assume that time is divided into *beacon intervals* that begin and end approximately at the same time at all nodes. A similar approach is also taken in [7].

The *power saving mechanism* specified for DCF requires that at the start of each beacon interval, every node must stay awake for a fixed time interval, called the *ATIM (Ad-hoc Traffic Indication Message) window*. Thus, during an ATIM window, all nodes are in the awake state. The ATIM window is utilized to announce any packets pending transmission to nodes in the doze state, as described later. An earlier investigation [55] shows that any fixed size of the ATIM window cannot perform well in all situations, when throughput and energy consumption are considered. This chapter presents an adaptive mechanism to dynamically adjust the size of the ATIM window. We refer to our protocol as Improved Power Saving Mechanism (IPSM). Note that IPSM allows different nodes to use different ATIM window sizes.

The rest of this chapter is organized as follows. Section A presents an overview of the DCF power saving mechanism in IEEE 802.11, and Section B reviews the related work. Our proposed approach, IPSM, is presented in Section C. Section D describes our simulation model and discusses the simulation results. Section E summarizes this chapter.

A. Power Saving Mechanism for DCF in IEEE 802.11

Fig. 1 illustrates the power saving mechanism (hereafter referred as PSM) in DCF. Time is divided into beacon intervals [23]. At the start of each beacon interval, each node stays

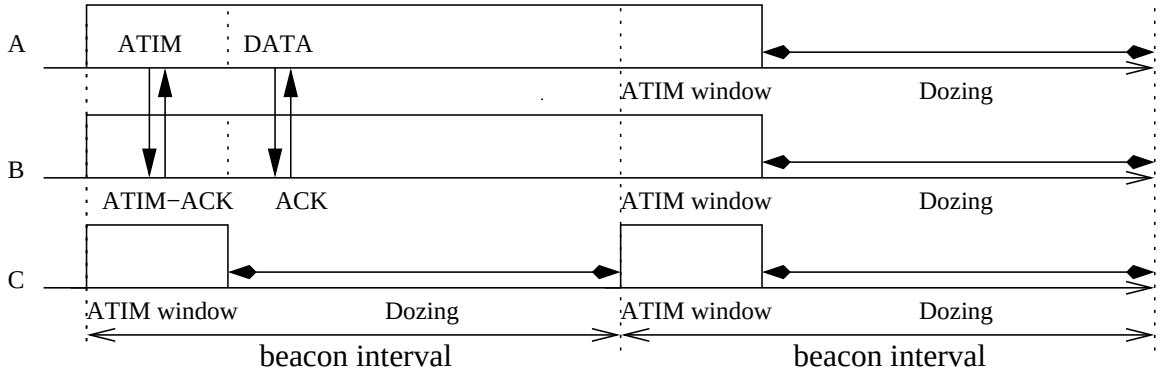

Fig. 1. Power saving mechanism for DCF: Node A announces a buffered packet for B using an ATIM frame. Node B replies by sending an ATIM-ACK, and both A and B stay awake during the entire beacon interval. The actual data transmission from A to B is completed during the beacon interval. Since C does not have any packet to send or receive, it dozes after the ATIM window.

awake for an ATIM window interval. We describe the power saving mechanism using Fig. 1. In PSM, when any node has a packet destined for another node, the packet is announced during a subsequent ATIM window. For instance, in Fig. 1, node A announces a packet destined for node B by transmitting an "ATIM frame" during the ATIM window. The transmission of an ATIM frame is performed using the CSMA/CA (collision avoidance) mechanism specified in IEEE 802.11. When a node has sent an ATIM frame to another node, such as node A in our example, the node remains awake for the entire beacon interval. A node that receives an ATIM frame replies by sending an ATIM-ACK. Such a node remains awake for the entire beacon interval, after transmitting the ATIM-ACK.

In our example, node B sends an ATIM-ACK to node A and remains awake for the rest of the beacon interval. Transmission of one or more data packets from node A to node B can now take place during the beacon interval, after the end of the ATIM window. A node that has no outstanding packets to be transmitted can go into the doze state at the end

of the ATIM window if it does not receive an ATIM frame during the ATIM window. In Fig. 1, node C dozes after the ATIM window, thus saving energy. All dozing nodes again wake up in PSM at the start of the next beacon interval.

In PSM specified in IEEE 802.11, all nodes use the same (fixed) ATIM window size, as well as identical beacon intervals [23]. Since the ATIM window size critically affects throughput and energy consumption, a fixed ATIM window does not perform well in all situations, as shown in [55]. If the ATIM window is chosen to be too small, there may not be enough time available to announce buffered packets (by transmitting ATIM frames), potentially degrading throughput. If the ATIM window is too large, there would be less time for the actual data transmission, since data is transmitted after the end of the ATIM window, again degrading throughput at high loads. Large ATIM windows can also result in higher energy consumption since all nodes remain awake during the ATIM window. In particular, at a low load, large ATIM windows are unnecessary. Thus, a static ATIM window size cannot always perform well. We propose a dynamic mechanism for choosing an optimal ATIM window size.

B. Related Work

As mentioned earlier, PCF in IEEE 802.11 [23] also supports a power saving mechanism. For power management in PCF, base stations periodically transmit *beacons*. A base station buffers packets for nodes in the doze state and these buffered packets are announced in a TIM (Traffic Indication Map). TIM is an element included in all beacons generated by a base station. A node in the sleep state periodically wakes up and listens for beacons. It transmits a PS-Poll (Power Save Poll) frame to the base station if the TIM indicates pending packets for the node. The base station then transmits the buffered packets to the node. A node can go back to the doze state if the TIM indicates that there is no pending packet for

the node.

Woesner *et al.* [55] present simulation results for the power saving mechanisms of two wireless LAN standards, IEEE 802.11 and HIPERLAN. They show the different sizes of beacon intervals and ATIM windows in IEEE 802.11 have significant impact on throughput and energy consumption. Tseng *et al.* [51] propose some solutions for synchronizing beacon intervals when using DCF in multi-hop wireless networks. Bluetooth [3] is designed for a low-cost and low-power wireless network. Bluetooth devices are usually organized into so called piconets, which consist of one master and up to 7 slave devices. Bluetooth provides three different low power modes (*sniff, hold* and *park*) to reduce energy consumption. Energy efficiency in Bluetooth is studied in [24, 61].

IEEE 802.11 uses a handshake consisting of RTS (Request-To-Send) and CTS (Clear-To-Send) preceding transmission of a data packet. A power-conserving algorithm proposed in [5] requires a node to enter the doze state if it overhears RTS/CTS for data transmission between some other nodes (the RTS and CTS packets specify duration of the impending data transfer, which can be used to determine the doze period). However, this approach is not always suitable due to the time and energy costs associated with a doze-to-active transition – these costs can make it expensive to transition between awake and doze states on a per-packet basis. Our scheme, on the other hand, makes transitions between awake and doze states at most once per beacon interval.

A power saving scheme presented in [9] is another variation of IEEE 802.11 PSM. The scheme has two time slots for beacon transmissions, called ETS (Earlier Time Slot) and LTS (Later Time Slot). When a node has a pending packet it transmits a beacon during ETS. In contrast, if no node has any pending packet, beacons will be transmitted during LTS. In this case, all nodes can enter the doze state after beacon transmissions to save energy. However, the scheme has a limitation. It uses almost a half of beacon interval (40 ms) for the ATIM window. Thus, when only one node in the network has a pending

packet during a beacon interval, the node will transmit a beacon during ETS. This results in a situation where all nodes stay awake for the long ATIM window (40 ms) wasting their energy. Moreover, large ATIM window gives less time for the actual data transmission.

SPAN [7], a power saving technique, elects a group of “coordinators” which are changed periodically. The coordinators stay awake and forward traffic for active connections. Non-coordinators follow the power saving mechanism in IEEE 802.11. Nodes buffer the packets for dozing destinations and announce these packets during ATIM window. SPAN introduces a new advertised traffic window following an ATIM window. During this advertised traffic window, the announced packets and the packets for the coordinators can be transmitted. After this window, only the packets for the coordinators can be transmitted, and non-coordinators can go to doze state if they do not have traffic to send or receive.

The protocol proposed in [60] also uses the power saving mechanism of IEEE 802.11. However, unlike IEEE 802.11, the protocol in [60] uses information from the network layer to reduce packet delivery latency. When a node receives routing packets, such as route request, route reply, etc., the node will stay awake for a predefined time duration, which is much longer than a beacon interval. Nodes involved in packet forwarding will be awake for a longer time, so that the end-to-end latency is reduced.

GAF [58] uses location information, provided by GPS, to form “virtual grids”. All nodes in the same grid are equivalent in terms of traffic forwarding. GAF guarantees that one node in each grid stays awake in order to forward traffic.

In PAMAS [47], each node uses two separate channels for control packet and data packet transmissions. Using the control channel, a node determines when to power off and the power-off duration. This scheme has the disadvantage of requiring two channels for communication. Similar to PAMAS, S-MAC [59] allows nodes to sleep during neighbors’ transmissions; nodes go to sleep after hearing an RTS or a CTS destined for neighbors.S-

MAC is designed for wireless sensor networks, where each node usually has limited energy capacity and limited wireless channel bandwidth. S-MAC reduces contention latency by *message passing*. Long messages are fragmented into many small fragments, which are transmitted in bursts. Only one RTS and one CTS are used to transmit many fragments. When nodes overhear an RTS or a CTS, they will go to sleep for the time that is needed to transmit all the fragments.

Another energy efficient protocol is proposed in [22] for wireless microsensor networks, where each node usually has limited energy capacity and limited wireless channel bandwidth. A cluster-based routing protocol, LEACH (Low-Energy Adaptive Clustering Hierarchy), is proposed to minimize global energy consumption by distributing the load to all the nodes.

C. Proposed IPSM Scheme

We now present our proposed scheme, IPSM (Improved Power Saving Mechanism). There are two main differences between IPSM and PSM specified in IEEE 802.11:

- *Dynamic adjustment of ATIM window*

  In the proposed IPSM scheme, each node independently chooses an ATIM window size based on observed network conditions. This might potentially result in each node using a different ATIM window size.

- *Longer dozing time (more energy saving)*

  In PSM specified in IEEE 802.11, when a node transmits or receives an ATIM frame during an ATIM window, it must stay awake during the entire beacon interval. This approach allows a single ATIM frame from, say node A to node B, to be followed up by multiple data packets during the remaining beacon interval – that is, a single ATIM frame and ATIM-ACK exchange can be used to deliver several packets in the same

beacon interval. While this approach has its advantages, at low loads, this approach results in a much higher energy consumption than necessary. In the proposed IPSM scheme, we allow a node to enter the doze state after completing any transmissions that are explicitly announced in the ATIM window.

For instance, if node A has only one packet pending, say, for node B, and no other node has a packet pending for node B, then both nodes A and B would enter the doze state after completing transmission of the single packet (when using IPSM) – on the other hand, with PSM in IEEE 802.11, both A and B will remain awake for the entire beacon interval. As noted above, IEEE 802.11 approach has the benefit of being able to transmit multiple packets to a destination following a single ATIM frame. IPSM achieves the same benefit of the IEEE 802.11 approach by piggybacking the number of pending packets inside data packets.

As we will see later, the first feature, dynamic adjustment of ATIM window, allows to achieve throughput comparable to that of IEEE 802.11 while the second feature results in saving more energy.

In IPSM, a node uses only one ATIM frame to announce pending packets for the same destination during the same beacon interval. When a node, say node A, successfully transmits an ATIM frame to another node, say node B, node A will not transmit another ATIM frame to the same destination in the same beacon interval. Instead, node A includes in each packet sent to B the number of packets still pending for node B[1]. This information allows node B to determine when it has received all the packets pending at node A at the time of data transmission. If node A could not deliver all pending packets that were

[1]In fact, there exists “more data” bit that can be used for the same purpose. That is, node A can set the “more data” bit inside data packets and B will stay awake until ”more data” is set to zero. In the simulation, we include the number of pending packets, however, using “more data” bit the protocol will become simpler.

previously announced to node B, and the current beacon interval expires, nodes A and B both stay up in the next beacon interval, with B anticipating the remaining packets from node A, without node A having to send an ATIM frame to node B. Node A delivers the remaining packets to B, and then may enter the doze state if it has no other announced pending packets to transmit or receive. Similarly, node B may enter the doze state after receiving the previously announced packets, if it is not aware of any other pending packets. Like PSM, if packets arrive after a node has already entered the doze state they will be buffered and announced during a subsequent ATIM window.

1. IPSM Protocol

In this subsection, we present the IPSM operations in detail. We first define few terms that are used in the rest of the chapter:

- *ATIMmin:* The minimum ATIM window size that a node can have. *ATIMmin* is set to 2 ms in our simulations.
- *ATIMmax:* The maximum ATIM window size that a node can have. *ATIMmax* is set to 16 ms.
- *ATIMinc:* The amount of time by which a node can increase the ATIM window at a time. *ATIMinc* is set to 2 ms.
- *CIT (Channel Idle Time):* Current channel idle time measured at the end of the ATIM window. During the ATIM window, each node measures how long the channel was idle continuously. Whenever the channel is busy the *CIT* value is reset to zero. Therefore, if the *CIT* value is greater than zero at the end of the ATIM window, it implies that the channel is idle at that time.
- *CITThreshold (Channel Idle Time Threshold):* At the end of the ATIM window if *CIT* is greater than *CITThreshold* the channel is idle long enough to assume that no

node intends to transmit an ATIM frame. Thus, in this case, a node does not need to increase its ATIM window size. *CITThreshold* is set to 128 time slots (2.56 ms) in our simulations. The reason why *CITThreshold* is chosen to be 128 time slots is described later.

Fig. 2 illustrates the IPSM scheme. At the beginning of each beacon interval, nodes transmit beacons, as described in IEEE 802.11. After that, each node begins with ATIM window size equal to *ATIMmin*. When the ATIM window finishes a node compares *CIT* with *CITThreshold*. If *CIT* is less than or equal to *CITThreshold* the node increases its ATIM window by *ATIMinc* and restarts the ATIM window for *ATIMinc*. For instance, in Fig. 2, node A and B transmit an ATIM and ATIM-ACK, respectively, during the ATIM window. At the end of the ATIM window, A, B, and C have *CIT* less than *CITThreshold*. Thus, they increase their ATIM window size by *ATIMinc*. This process is repeated until *CIT* exceeds *CITThreshold*, or until the ATIM window size reaches *ATIMmax*[2]. After the ATIM window finishes, nodes begin their data transmissions. When they complete their packet transmissions they enter the doze state. In our example, A and B start their data transmission after the increased ATIM window finishes. After completing data transmissions, they start dozing for the remaining beacon interval. Since C has no packet to send or receive, it dozes after the ATIM window. All nodes wake up at the start of the next beacon interval, and repeat the process. That is, every node transmits a beacon and starts its ATIM window size equal to *ATIMmin*. Since no node in Fig. 2 has a packet to send or receive, A, B, and C will have *CIT* greater than *CITThreshold* at the end of the ATIM window (*ATIMmin*). Hence, they can enter the doze state for the rest of beacon interval. Pseudo code for adjusting the ATIM window is described in Algorithm. 1.

[2]As an alternative to increase the ATIM window size by *ATIMinc*, a node may continue in the ATIM window until its *CIT* value exceeds *CITThreshold* or the ATIM window size reaches *ATIMmax*. Using this alternative the protocol will become simpler.

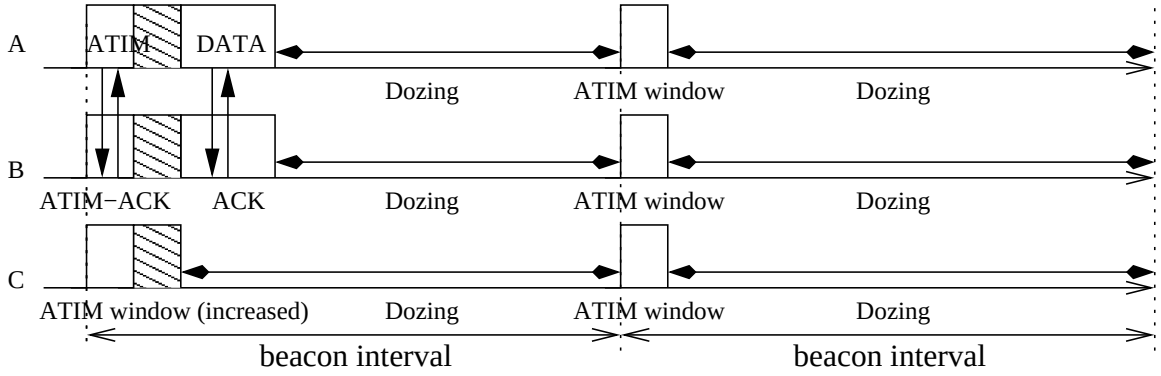

Fig. 2. IPSM: During the ATIM window node A and B transmit an ATIM and ATIM-ACK, respectively. At the end of the ATIM window, *CIT* is less than *CITThreshold*. Thus, nodes A, B, and C increase their ATIM window size by *ATIMinc*. When the increased ATIM window finishes nodes have *CIT* larger than *CITThreshold*, so A and B start their data transmission. Since C has no packet to send or receive it dozes after the ATIM window. Once completing all the data transmission A and B will also doze for the remaining beacon interval.

Note that there exists a finite delay associated with the doze-to-awake transition as well as a higher energy consumption. Therefore, in IPSM, a node will not enter the doze state after completing packet transmissions if the remaining duration in the current beacon interval is "too small" – specifically, in our simulations, a node will not enter the doze state if the remaining duration is less than 1600 μs – the delay for both doze-to-awake transition and awake-to-doze state transition are assumed to be 800 μs each [21, 45].

We now explain the reason why we set *CITThreshold* to 128 time slots. As mentioned earlier, each ATIM frame is transmitted using the CSMA/CA mechanism in IEEE 802.11. Specifically, a node wanting to transmit an ATIM frame picks a backoff interval in the range $[0, cw]$, where cw denotes the *contention window*. The initial cw value is called $cwmin$. The backoff interval is decremented by 1 after each "clock tick" if the channel is sensed as

Algorithm 1 IPSM: ATIM Window Adjustment

```
1: ATIM window is set to ATIMmin;
2: finished := false;
3: repeat
4:    if ATIM window expired then
5:       Node checks its CIT;
6:       if CIT ≤ CITThreshold and ATIMsize < ATIMmax then
7:          Continue in ATIM window for ATIMinc duration;
8:       else
9:          Start data transmission or enter the doze state;
10:         finished := true;
11:      end if
12:   end if
13: until finished is true;
```

idle [23]. An ATIM frame is transmitted when the backoff interval reaches 0. When the ATIM frame is received by the destination node, it responds by sending an ATIM-ACK. However, the ATIM frame may collide with an ATIM frame transmitted by another node. In this case, the ATIM-ACK will not be sent. If an ATIM-ACK is not received in response to the transmitted ATIM frame, the node transmitting the ATIM frame doubles the value of cw, selects a new backoff interval, and repeats the process to retransmit the ATIM frame. In IPSM, a node can retransmit an ATIM frame up to 3 times for the same destination. Therefore, when $cwmin$ is 31 the cw value can be doubled up to 128. This means that if the *CIT* value at the end of the ATIM window is larger than 128 time slots we can assume that no node has an ATIM frame to transmit. Therefore, nodes stop increasing their ATIM window sizes and start their data transmission when *CIT* is greater than *CITThreshold*.

2. Hidden and Exposed Terminal Problems

The IPSM protocol may have the exposed terminal problem due to the CSMA mechanism. In this subsection, we first explain the hidden and exposed terminal problems in wireless network, and show how the exposed terminal problem can affect IPSM. After that we propose some solutions to overcome the problem.

Fig. 3 (a) and (b) illustrate the hidden and exposed terminal problems, respectively. In Fig. 3 (a), node A wants to send a packet to node B and node C wants to send a packet to node D. When A sends a packet to B, C cannot hear it so C will assume the channel to be idle. Therefore, when C starts to send a packet to D it will cause a collision at B. This is called the hidden terminal problem – that is, A is "hidden" for C. The hidden terminal problem can cause more collisions, wasting channel bandwidth.

The exposed terminal problem is depicted in Fig. 3 (b). When B sends a packet to A, C has to defer its transmission to avoid a collision at B. Therefore, when D sends a packet to C, C will not respond to D. This is called the exposed terminal problem – that is, C is "exposed" to B. While the hidden terminal problem results in data loss, the exposed terminal problem reduces efficiency.

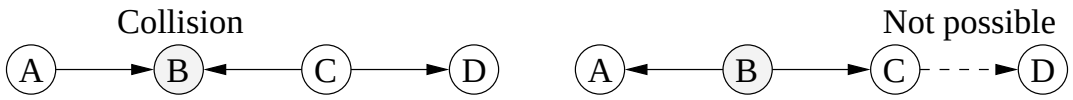

(a) Hidden terminal problem (b) Exposed terminal problem

Fig. 3. (a) Node A is transmitting a packet to node B; node A is "hidden" for node C. When C starts to transmit a packet to node D, it will cause a collision at B. (b) Node B is transmitting a packet to node A. Since node C is "exposed" to B, node B has to defer its transmission with node D. While the hidden terminal problem results in data loss, the exposed terminal problem simply reduces efficiency.

IPSM has the exposed terminal problem during the ATIM window. Recall that the AITM window in IPSM expires when the channel is idle for 128 slot time. Let us consider the scenario in Fig. 3 (b). Suppose A and B communicate ATIM and ATIM-ACK with each other, and C wants to send an ATIM to D. While C is deferring its transmission for B, D will sense the channel to be idle and its idle timer may pass 128 slot time. Thus, D will finish its ATIM window and enter the doze state without receiving packets from C.

To overcome this problem, we propose a simple solution. In IPSM, if a node cannot transmit an ATIM, it will choose a small cw value (15 in the simulation) in the subsequent beacon interval. If an ATIM-ACK is not received in response to the transmitted ATIM frame, retransmission occurs using the CSMA/CA mechanism. That is, the node transmitting the ATIM frame doubles the value of cw, selects a new backoff interval, and repeats the process to retransmit the ATIM frame. Since the $cwmin$ value is 31 the node can send its ATIM frame earlier than other nodes with a high probability. This is not a perfect solution for the exposed terminal problem, but as we will show it works reasonably well. A more solid solution to the exposed terminal problem can be using a separate busy tone channel. In our example in Fig. 3 (b), when node C receives packet from B it defers its transmission to D. Using a busy tone channel, C can transmit busy tones to D so that node D can sense it [36]. By this way, D will know the existing transmission and will not enter the doze state. In this dissertation, we adopt the solution using small cw, which is simpler than using busy tones.

3. Power Saving Mode with TCP

TCP (Transport Control Protocol) is a connection-oriented, reliable data delivery protocol. For congestion control, TCP uses a congestion window ($cwnd$) at a sender, which indicates the amount of data that can be injected into the network. TCP assumes that network is congested when it fails to receive an acknowledgment for a packet within some retransmission

timeout (RTO) interval. RTO is determined by estimating the mean and variance of the RTT (Round Trip Time). When packet loss is detected, lost packets are retransmitted. At this time, the sender decreases the congestion window to avoid further congestion. Thus, the amount of data being transmitted at the sender is reduced. On the other hand, whenever the sender receives an acknowledgment, it increases the congestion window to transmit more data. Congestion window threshold is set to half of the congestion window size if packet retransmission is required.

As we will see in Section D. 2, power saving mode in PSM or IPSM does not perform well with TCP. In PSM, if the ATIM window is too small some nodes may not be able to announce their buffered packets. When the nodes enter the doze state for a few beacon intervals, the TCP timeout occurs and packets are retransmitted. This will affect the TCP performance. On the other hand, if the ATIM window is too large there is a delay for a sender to receive acknowledgments from its receiver. Thus, the congestion window will be increased slowly, which affects the amount of data transmission and the TCP performance. However, we observe that having the ATIM window itself also delays a sender to receive acknowledgments. This makes the congestion window increase slowly, which causes the TCP throughput degradation.

The TCP throughput of IPSM may be worse than that of PSM because a node can enter the doze state in the middle of a beacon interval. This feature gives good energy savings for CBR (Constant Bit Rate) but not for TCP because it reduces time for data transmission.

Since the TCP throughput is degraded with any power saving mode, in this dissertation, we allow IPSM to give up power saving mode when there is TCP traffic in the network – that is, nodes will stay awake if there is TCP traffic. We refer to this as IPSM-T (IPSM for TCP). In IPSM-T, each node maintains a time-to-alive timer. When a node sends or receives a TCP packet it sets the timer for a predefined interval (200 ms in our simulation). The node will not enter the doze state as long as the timer is not zero. Furthermore, when a

sender transmits TCP packets, it indicates TCP traffic using one bit (say, TCP flag) inside the packet headers of ATIM, RTS, and DATA. Similarly, when a receiver receives TCP packets, it sets the TCP flag to 1 inside the packet headers of ATIM-ACK, CTS, and ACK. Therefore, when neighbor nodes overhear these packets they look at the packet header and check if the TCP flag is 1. If so, they update their time-to-alive timers and will not enter the doze state. As long as there exists a TCP flow in the network, the timer at each node is updated so that nodes involved in the TCP traffic can stay awake. Although all nodes in IPSM-T maintain beacon intervals, they will not transmit beacons if the timer is not zero. Also, a node will not transmit an ATIM since it assumes the destination is awake. On the other hand, when the timer is zero, nodes assume that there is no TCP traffic so they transmit beacons and ATIM frames. Note that each node performs this process independently. Therefore, there can be some nodes that do not involve TCP traffic nor overhear the traffic. These nodes will use power saving mode and enter the doze state after their ATIM windows finish. A similar approach that uses a keep-alive timer is also taken in [60], where nodes stay awake for a predefined time duration if they receive routing packets, such as route request, route reply, etc.

D. Performance Evaluation

We simulate the proposed IPSM scheme, the PSM scheme in IEEE 802.11, and IEEE 802.11 without any nodes in the power saving mode – we refer to the last one as With-Out Power Saving Mechanism (WOPSM). For IPSM, since there are two features that are different from PSM (dynamic ATIM window and sleeping after finishing packet transmission), we also simulate a scheme that has each feature. We refer to these as PSMD (PSM with the dynamic ATIM window option), and PSMS (PSM with the sleeping early option). As we will see, having the dynamic ATIM window leads to optimal throughput and having

the sleep option leads to more energy savings.

We use two metrics to evaluate the proposed scheme:

- *Aggregate throughput over all flows in the network*: One of our goals is to design an energy conserving MAC protocol that improves energy consumption without degrading throughput. Therefore, this metric is useful to measure if any throughput degradation occurs when using the proposed scheme.
- *Total data delivered per unit of energy consumption (Kbits delivered per joule)*: This metric measures the amount of data delivered per joule of energy. It is obtained by dividing the aggregate throughput over all flows by total energy consumption over all nodes in the network. Total energy consumption is the sum of each node's energy consumption during the simulation time. We use this metric as a measurement of energy consumption – the greater the value of this metric, the lower the energy consumption.

  We do not use total energy consumption over a simulation duration as a metric because the amount of useful "work" done (i.e., throughput achieved) by different schemes over a given amount of time may be different. For instance, some scheme may consume very little energy but also achieve very little throughput. Thus, it is not fair to compare energy consumption of different schemes over a fixed time interval. Therefore, we use the total data delivered per joule metric.

1. Simulation Model

We use ns-2 with the CMU wireless extensions [10] for our simulations. The channel bit rate is 2 Mbps, and the packet size is fixed at 1000 bytes. The duration of each simulation for UDP is 20 seconds. Each flow transmits Constant Bit Rate (CBR), and the rate of CBR traffic is varied in different simulations. For TCP simulations, we use on-off traffic; The *on*

and *off* intervals for each period is 10 and 100 seconds, respectively [60]. The simulation time is set to 400 seconds. Each flow transmits TCP traffic, which is generated by FTP applications.

For the energy model, we use 1.65 W, 1.4 W, 1.15 W, and 0.045 W to represent the power consumed by the wireless network interface in the transmit, receive, and idle modes and the doze state, respectively. For a doze to awake transition time, we use 800 μs [21, 45], which is a much more conservative estimate than 250 μs in [27]. During this transition time, a node consumes twice the power of idle mode.

Each node starts with enough energy so that it will not run out of its energy during the simulations. All the simulation results are averages over 30 runs. We use 100 ms for each beacon interval [23]. We simulate WOPSM, PSM, IPSM, PSMD, and PSMS. For PSM and PSMS simulations, we vary the ATIM window size from 4 ms to 40 ms.

a. Wireless LAN

For a Wireless LAN, the number of nodes is chosen to be 10, 30, or 50. In all cases, half of the nodes transmit packets to the other half. Therefore, when the number of nodes is n, there is a total of $\frac{n}{2}$ flows in the network.

With CBR traffic, we vary the total network load to observe the effect of network load on throughput and energy consumption. Simulated network loads are 10%, 20%, 30%, 40%, and 50%, measured as a fraction of the channel bit rate of 2 Mbps. For example, at a network load of 10%, the total bit rate of all the traffic sources is $0.1 \times 2 = 0.2$ Mbps. Each traffic source has the same bit rate. Thus, with a total load of 10%, and with 10 traffic sources, each traffic source has a rate of 0.02 Mbps. We also simulate each scheme with a dynamic network load using CBR. As Fig. 4 shows, the source nodes start with a network load of 40% and the network load changes from 40% to 10% at 5 seconds. The nodes then change from 10% to 20%, and from 20% to 30% at 5 second intervals.

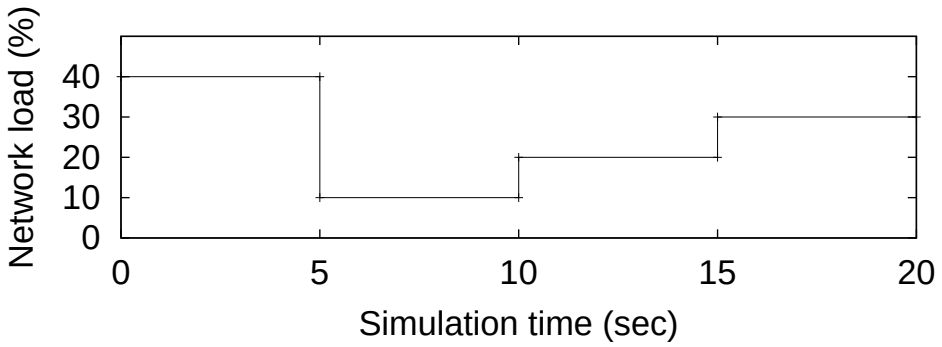

Fig. 4. In our dynamic network load scenario, the network load changes as the simulation time changes.

b. Random Topology

For the multi-hop network, 50 nodes are randomly placed in a 1000 x 1000 m^2 area. Ten source and ten destination nodes are randomly chosen. Note that a source or destination node can also be an intermediate node that forwards traffic for other nodes. The average route length of the flows is 3 hops with a range of 1 to 5 hops. For CBR traffic, each traffic source generates data rate of 5, 10, 15, or 20 Kbps. For TCP traffic, we use on-off traffic; The *on* and *off* intervals for each period is 10 and 100 seconds, respectively. The simulation time is set to 400 seconds.

2. Simulation Results

We now present simulation results. The following abbreviations are used to describe protocols used in graphs in this chapter:

- *WOPSM:* IEEE 802.11 WithOut Power Saving Mode.
- *PSM:* IEEE 802.11 Power Saving Mode.
- *IPSM:* Improved PSM, our proposed scheme.

In IPSM, since there are two features that are different from PSM (dynamic ATIM window and sleeping after finishing packet transmission) we simulate a scheme that has only one feature so that we can observe how each feature affects throughput and energy savings. For these schemes, we use the following abbreviations:

- *PSMS:* PSM with the Sleeping early option.
- *PSMD:* PSM with the Dynamic ATIM window. PSMD adjusts the ATIM window size using the channel idle time like IPSM.

Although the purpose of the power saving technique is to save as much energy as possible, we would like it to not degrade throughput. Thus, the goal is to use an ATIM window size that leads to high energy savings without degrading throughput.

When a node is in the doze state, it can save 1.105 joule of energy per 1 second of dozing time, since the power consumption difference between the idle mode and the doze state is 1.105W (1.15W − 0.045W). However, there is also energy loss due to the overhead of sending beacons, ATIM, and ATIM-ACK frames. Whenever a node transmits these packets, it will consume the power of the transmit mode, and the neighbor nodes will consume the power of the receive mode. Therefore, we have to make sure that the energy gain from the doze state is larger than the energy loss.

a. Wireless LAN: Fixed Network Load

This subsection presents simulation results in the case where the total network load is constant throughout the simulation. Figs. 5, 6, 7, and 8 show simulation results for fixed network loads in a Wireless LAN.

Fig. 5 shows the aggregate throughput (aggregated over all flows) with fixed network loads when using PSM, IPSM, and WOPSM schemes. In these figures, letter I on the horizontal axis corresponds to the proposed IPSM scheme, and letter W corresponds to

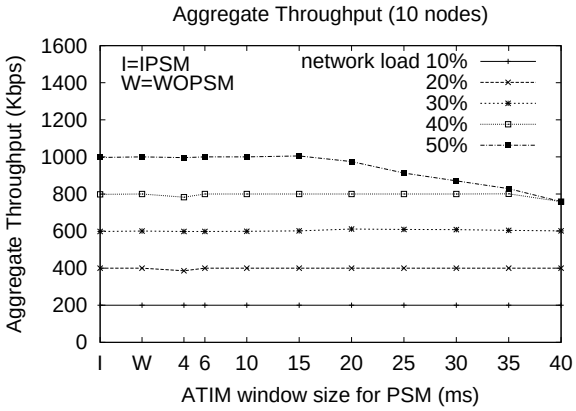

(a) Aggregate throughput (10 flows)

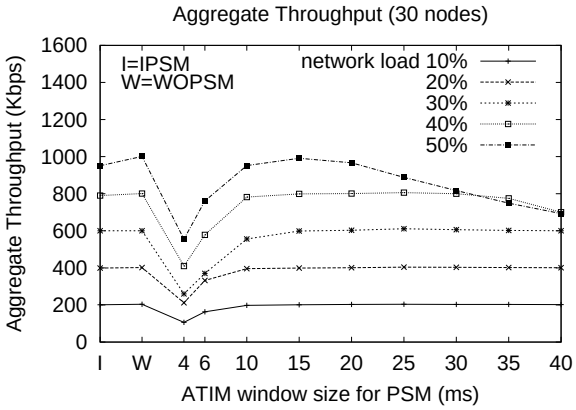

(b) Aggregate throughput (30 flows)

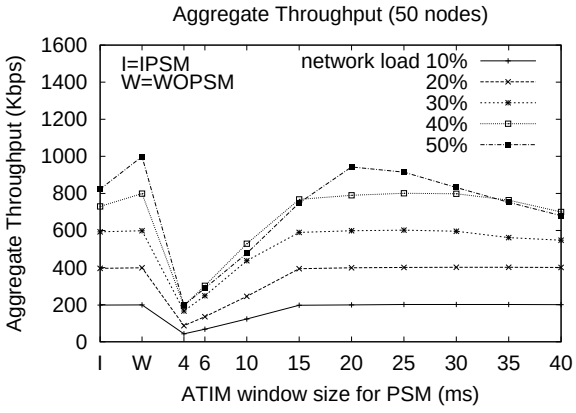

(c) Aggregate throughput (50 flows)

Fig. 5. Aggregate throughput: fixed network load.

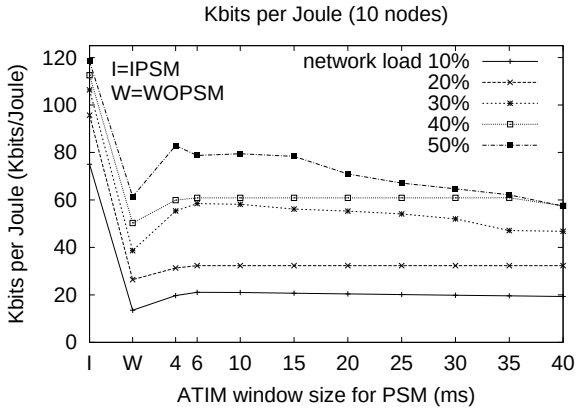

(a) Total data delivered per joule (10 flows)

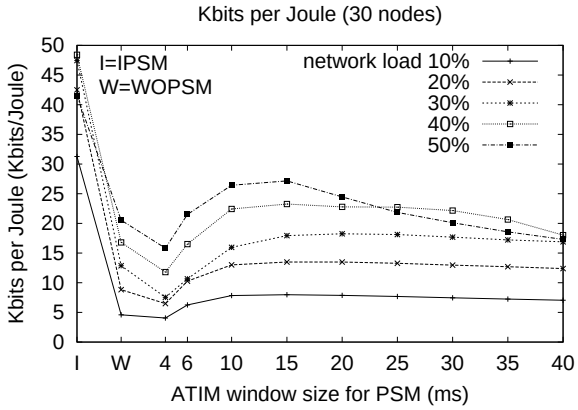

(b) Total data delivered per joule (30 flows)

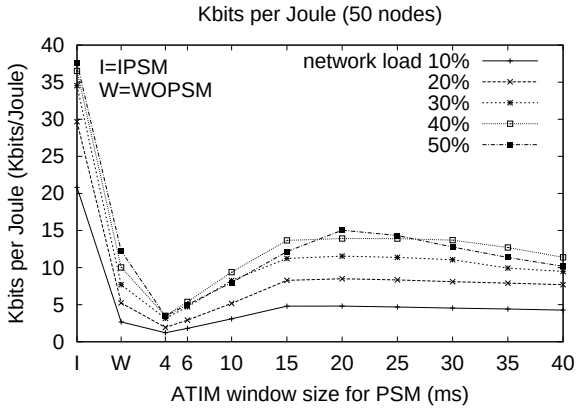

(c) Total data delivered per joule (50 flows)

Fig. 6. Total data delivered per joule: fixed network load.

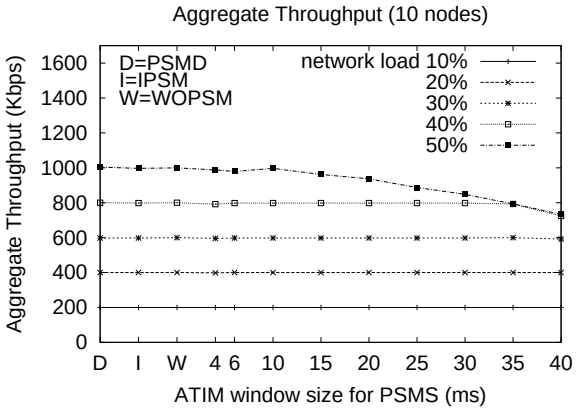

(a) Aggregate throughput (10 nodes)

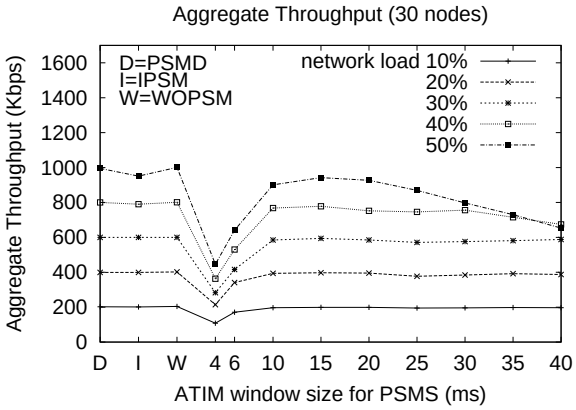

(b) Aggregate throughput (30 nodes)

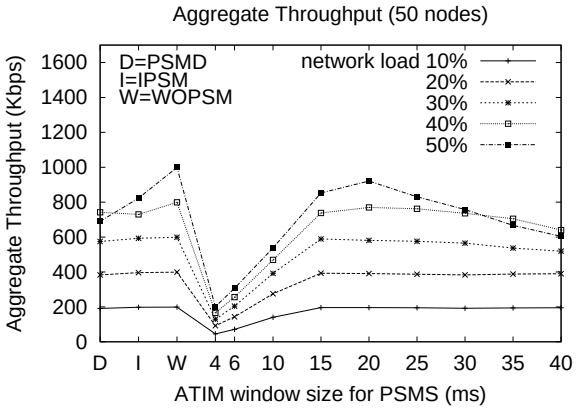

(c) Aggregate throughput (50 nodes)

Fig. 7. Aggregate throughput: fixed data rate (PSMS)

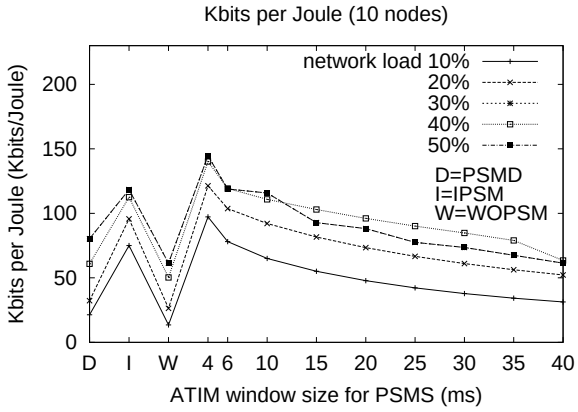

(a) Total data delivered per joule (10 nodes)

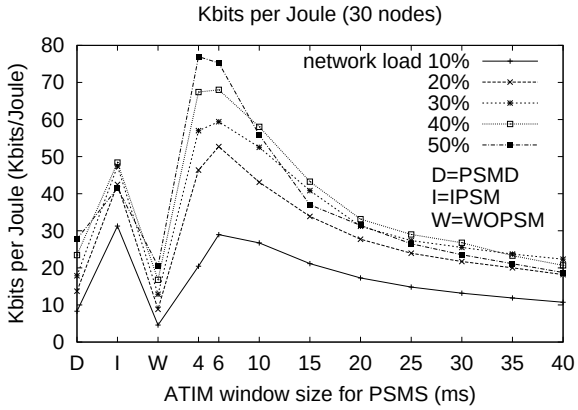

(b) Total data delivered per joule (30 nodes)

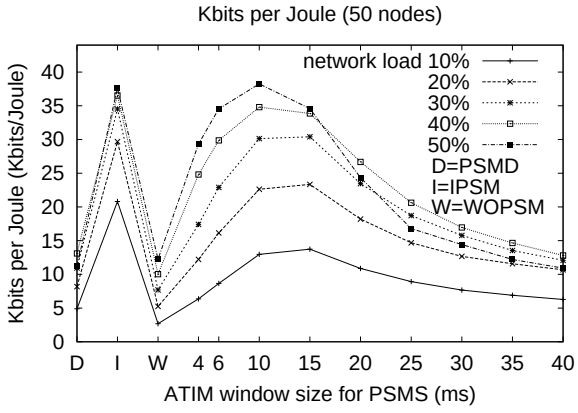

(c) Total data delivered per joule (50 nodes)

Fig. 8. Total data delivered per joule: fixed data rate (PSMS)

the WOPSM scheme. The performance of the PSM scheme in IEEE 802.11 depends on the chosen ATIM window value. The figure plots the throughput of PSM as a function of the ATIM window size. The ATIM window sizes are varied between 4 ms and 40 ms, as plotted on the horizontal axis. The results in Fig. 5(a), (b), and (c) are for different numbers of nodes on the LAN.

As the graphs show, the ATIM window size affects throughput achieved by PSM quite significantly, especially with a large number of nodes in the network (Fig. 5 (c)). On the other hand, proposed IPSM typically yields throughput comparable to WOPSM and PSM with the optimal value of ATIM window size. Also, IPSM typically conserves more energy than PSM, as we will discuss later in Fig. 6.

Recall that in PSM (and IPSM), each node only transmits one ATIM frame for many pending packets for the same destination. Thus, with a small number of nodes in the network, the ATIM window size for PSM is less sensitive in Fig. 5 (a) as compared to that in Fig. 5 (c). For example, in Fig. 5 (a), a 4 ms ATIM window is enough to achieve the desirable throughput for a network load of 10%. However, with a network load of 50% in Fig. 5 (c), an ATIM window of about 20 ms gives the best throughput. As the number of nodes increases or the network load gets heavier, the ATIM window size becomes a significant factor for both throughput and the energy consumption in PSM. If the ATIM window is too small, there is not enough time to announce all the pending packets, resulting in throughput degradation. If the ATIM window is too large, there is less time for the actual data transmission, resulting in throughput degradation as well. Aggregate throughput is also degraded in both PSM and IPSM with a network load of 50% in Fig. 5 (c). This is because the highly loaded network needs more time for data transmission, but both PSM and IPSM use the extra channel capacity for the ATIM window. Also, PSM with a 20 ms ATIM window performs a bit better than IPSM. In IPSM, nodes use more channel bandwidth than PSM since they have to wait for the channel to be idle for 128 time slots in order to finish

the ATIM window. Moreover, as long as there exists a node that sends an ATIM frame, the ATIM window size gets increased. If there are too many nodes that want to send an ATIM, it may result in a situation where there is no time for the actual data transmission. Thus, the ATIM window size in IPSM is not increased beyond *ATIMmax*, which is set to 16 ms in our simulations. It may be desirable to give up the power saving mode in a highly loaded network.

Fig. 6 shows the total data delivered per joule. IPSM performs better than PSM. Since all nodes are always awake with WOPSM, there is no energy savings from the doze state. Although PSM allows a node to be in the power saving mode, the node cannot enter the doze state if it has at least one packet to transmit or receive. This is a disadvantage when the network load is low. In IPSM, a node can enter the doze state whenever it finishes the transmission. This allows nodes to be in the doze state longer than PSM, leading to reduced energy consumption as compared to PSM.

When the network load increases or the number of nodes increases, energy savings from the power saving mode become smaller. For instance, the total data delivered per joule in the 30 and 50 node networks (Fig. 6 (b) and (c), respectively) are less than that in the 10 node network (Fig. 6 (a)). Note that the scales for the vertical axis in Fig. 6 (a), (b), and (c) are not identical. When the network load is high, there is less time for a node to be in the doze state due to data transmissions. Also, when the number of nodes in the network is large, there can be more collisions among the nodes. Therefore, a node will take more time to finish data transmission; hence, it is more likely to stay in the awake state. The shorter duration in the doze state will yield less energy conservation.

Figs. 7 and 8 show simulation results for PSMS and PSMD, respectively. Recall that IPSM combines PSMS and PSMD; the reason we simulate PSMS and PSMD is to show that each feature affects on energy savings and optimal throughput, respectively. Fig. 7 (a), (b), and (c) show the aggregate throughput with fixed network loads when using PSMD,

PSMS, IPSM, and WOPSM schemes for different numbers of nodes on the LAN. In these figures, letters D, I, and W on the horizontal axis correspond to the PSMD, IPSM, and WOPSM schemes, respectively. The performance of the PSMS scheme in IEEE 802.11 depends on the ATIM window size. The figure plots the throughput of PSMS as a function of the ATIM size. As in Fig. 5, the ATIM sizes are varied between 4 ms and 40 ms, as plotted on the horizontal axis.

PSMS is the same as PSM except that it allows for nodes to enter the doze state once they complete all transmissions that are announced during the ATIM window, which will affect primarily energy consumption. Thus, the aggregate throughput achieved by PSMS in Fig. 7 is similar to that in Fig. 5. Like PSM, the ATIM window size for PSMS is less sensitive with a small number of nodes in Fig. 7 (a) as compared to that in Fig. 7 (c).

PSMD works like PSM except that in PSMD the ATIM window size is dynamically adjusted as in IPSM. The aggregate throughput achieved by PSMD is similar to that achieved by PSM with an optimal ATIM window except at a very high load. With a network load of 50% in Fig. 7 (c), PSMD performs worse than that of PSMS with an optimal ATIM window or IPSM. PSMD performs worse than PSMS since it uses extra bandwidth for waiting for the channel to be idle in order to finish the ATIM window. Also, PSMD performs slightly worse than IPSM. In IPSM, nodes will not transmit an ATIM if they have not finished transmitting all the announced packet during the previous beacon interval, which allows to utilize less bandwidth for ATIM window and more bandwidth for data transmission as compared to PSMD.

In Fig. 8 PSMD does not save energy as compared to IPSM or PSMS. This confirms that the energy savings of IPSM mainly comes from entering the doze state after completing data transmission. The energy efficiency of IPSM is comparable to that of PSMS with an optimal ATIM window that leads to the maximum aggregate throughput in Fig. 7. The energy savings of PSMS gets decreased as the ATIM window size increases; with a large

ATIM window, there is less time for nodes to stay in the doze state. With a high network load in Fig. 8 (b), PSMS with an ATIM window of 4 ms saves much more energy than that of IPSM. However, the aggregate throughput achieved by PSMS with a 4 ms ATIM window is very low in Fig. 7 (b). With a small ATIM window only few nodes can transmit ATIM frames so using PSMS most nodes will power off their network interfaces and enter the doze state.

b. Wireless LAN: Dynamic Network Load

We now present simulation results for the wireless LAN where the load is time-varying. The dynamic network load used in these simulations is shown in Fig. 4, as discussed previously. Figs. 9 and 10 plot the aggregate throughput and the corresponding total data delivered per joule for IPSM (label I on horizontal axis), WOPSM (label W), and PSM schemes (with different values of fixed ATIM window size for PSM). Figs. 11 and 12 plot the aggregate throughput and the corresponding total data delivered per joule for IPSM (label I on horizontal axis), WOPSM (label W), PSMD (label D), and PSMS schemes (with different values of fixed ATIM window size for PSMS). The simulation results are similar to those for fixed network loads.

In Fig. 9 (a) and (b), ATIM windows of 5 ms and 10 ms in PSM give comparable throughput to IPSM and WOPSM, respectively. However, the corresponding throughput per joule is lower than that of IPSM in Fig. 10 (a) and (b). As discussed earlier, since the ATIM window size affects both throughput and energy consumption, PSM does not perform well all the time. This suggests that the ATIM window size should be dynamically adjusted according to the number of nodes contending in the network and the network load. The simulation using a dynamic network load shows that IPSM always performs well as compared to PSM.

Figs. 11 and 12 show simulation results for PSMS and PSMD using the dynamic

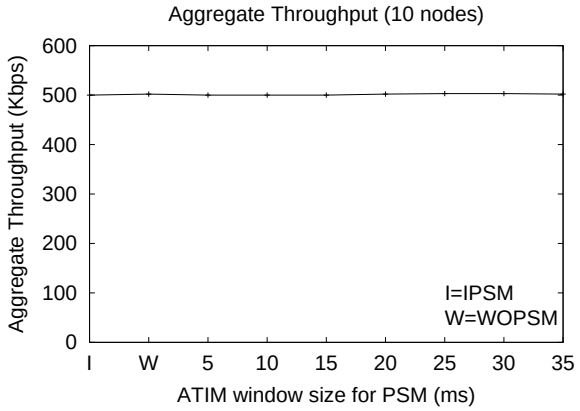

(a) Aggregate throughput (10 flows)

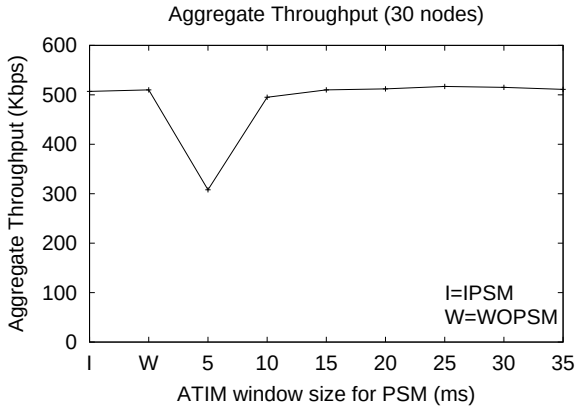

(b) Aggregate throughput (30 flows)

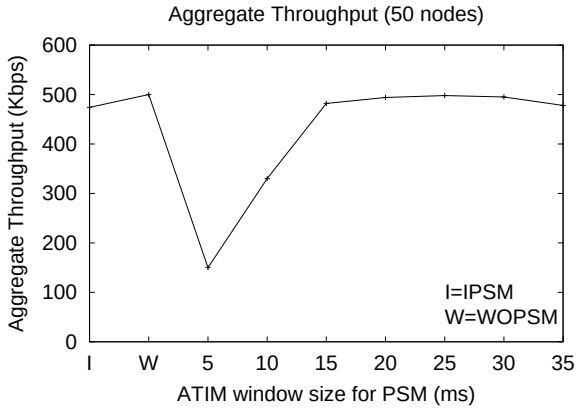

(c) Aggregate throughput (50 flows)

Fig. 9. Aggregate throughput: dynamic network load.

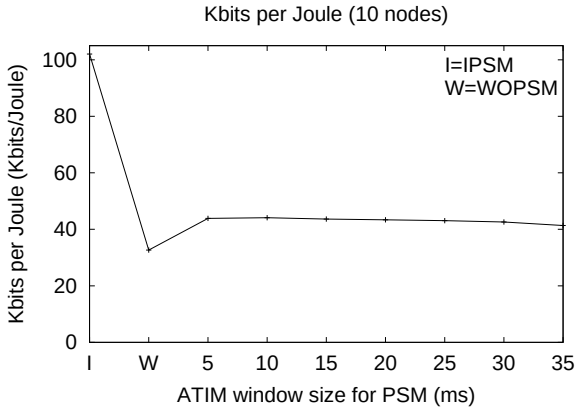

(a) Total data delivered per joule (10 flows)

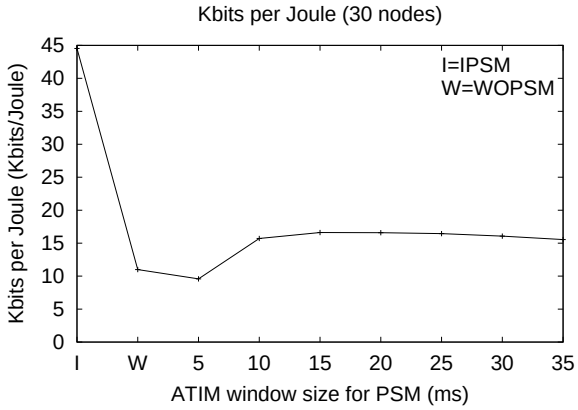

(b) Total data delivered per joule (30 flows)

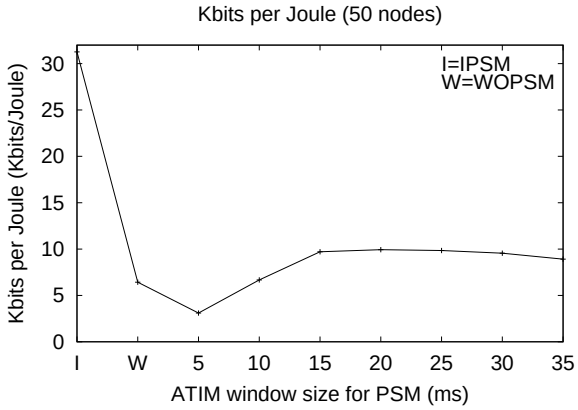

(c) Total data delivered per joule (50 flows)

Fig. 10. Total data delivered per joule: dynamic network load.

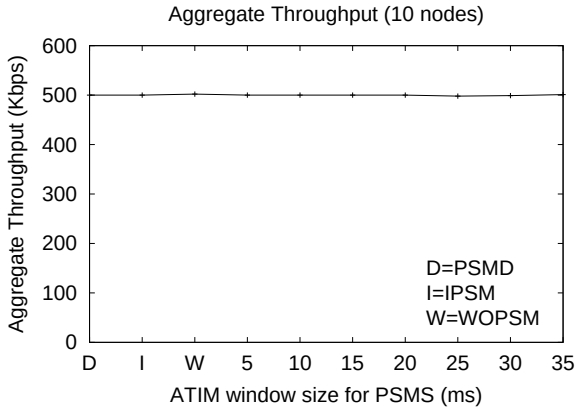

(a) Aggregate throughput (10 nodes)

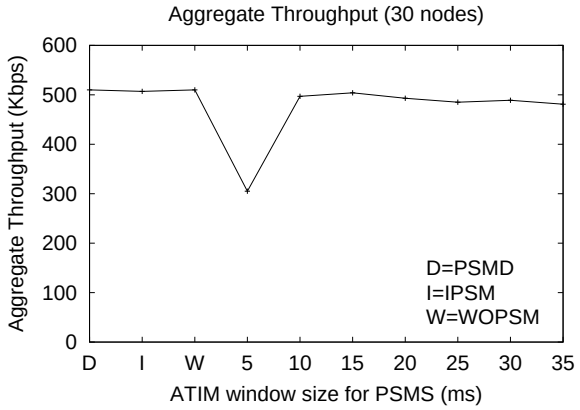

(b) Aggregate throughput (30 nodes)

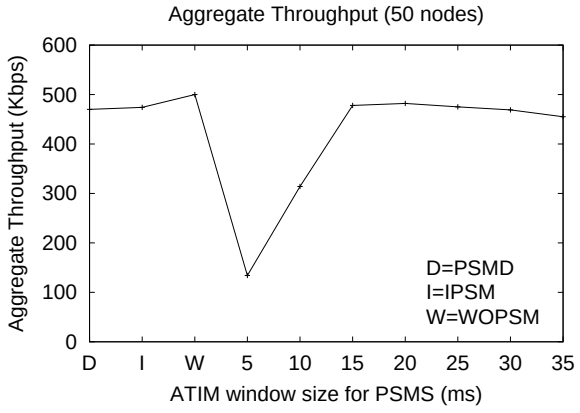

(c) Aggregate throughput (50 nodes)

Fig. 11. Aggregate throughput: dynamic rate (PSMS)

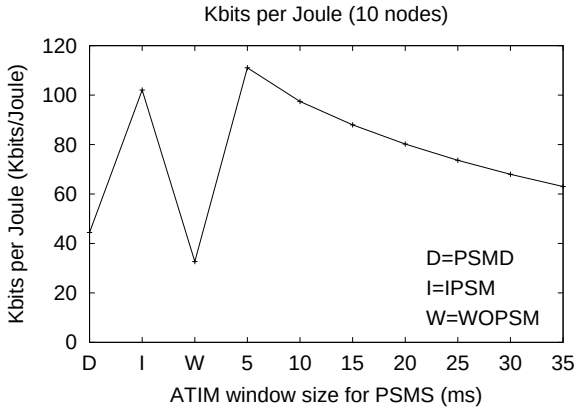

(a) Total data delivered per joule (10 nodes)

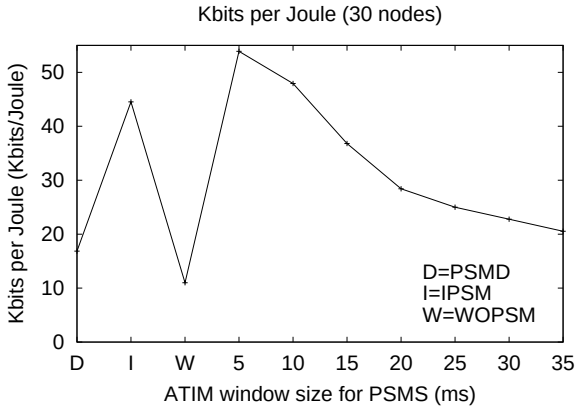

(b) Total data delivered per joule (30 nodes)

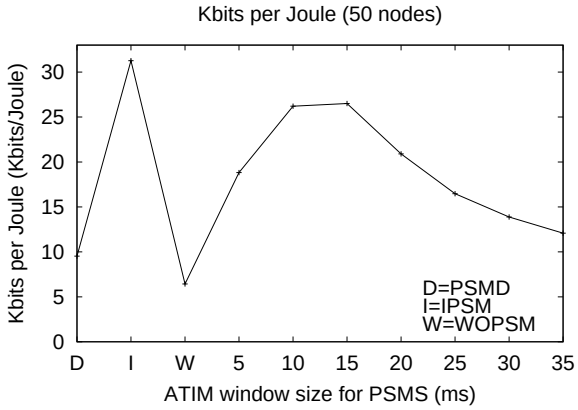

(c) Total data delivered per joule (50 nodes)

Fig. 12. Total data delivered per joule: dynamic rate (PSMS)

network load. The aggregate throughput of PSMD or IPSM is similar to that of PSMS with an optimal ATIM window size. The ATIM window size of PSMS is insensitive with a small number of nodes (Fig. 11 (a)) but a larger ATIM window is needed with a large number of nodes in the network (Fig. 11 (c)). Fig. 12 shows that PSMD does not conserve energy as compared to IPSM or PSMS. IPSM achieves energy savings comparable to that of PSMS with the optimal ATIM window size.

c. Random Topology: CBR Traffic

Figs. 13 (a) and 14 (a) show the aggregate throughput for IPSM (label I on horizontal axis), WOPSM (label W), PSMD (label D), PSM and PSMS (with different values of fixed ATIM window size for PSM and PSMS) for the multi-hop network case. Figs. 13 (b) and 14 (b) show the corresponding total data delivered per joule, respectively. In a multi-hop network, a packet may traverse several hops to reach a destination. An intermediate node using the power saving mode has to stay awake in order to forward the packet to the destination. This may result in more energy consumption compared to the wireless LAN case.

Simulation results for the multi-hop network are similar to those for the wireless LAN (see Figs 5–8). Although the aggregate throughput achieved by all schemes looks similar in Fig. 13 (a), IPSM yields the best energy savings among all schemes in Fig. 13 (b). In Fig. 14, PSMD achieves a comparable throughput as IPSM or PSMS, but it does not save energy as much. IPSM and PSMS achieve similar energy savings.

d. Random Topology: TCP Traffic

Figs. 15 and 16 show simulation results for TCP traffic. Letter T on the horizontal axis corresponds to IPSM-T, which allows IPSM to give up power saving mode when there is TCP traffic in the network – that is, nodes will stay awake if there is TCP traffic.

Both IPSM and PSMS in Fig. 15 (a) performs worse than WOPSM. Both schemes

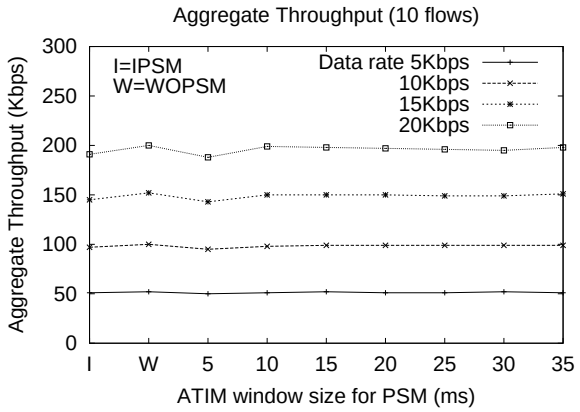

(a) Aggregate throughput (10 flows)

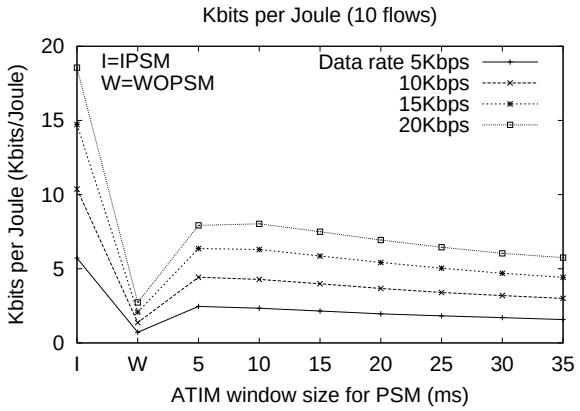

(b) Total data delivered per joule (10 flows)

Fig. 13. Random topology: 50 nodes with 10 udp flows

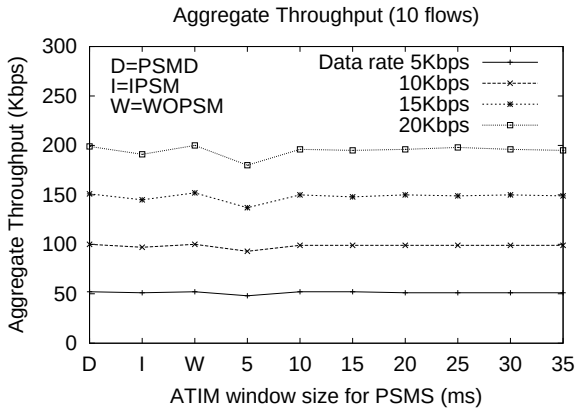

(a) Aggregate throughput (10 flows)

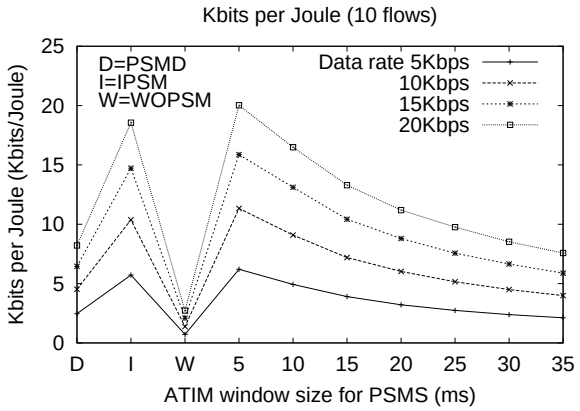

(b) Total data delivered per joule (10 flows)

Fig. 14. Random topology: 50 nodes with 10 udp flows (PSMS)

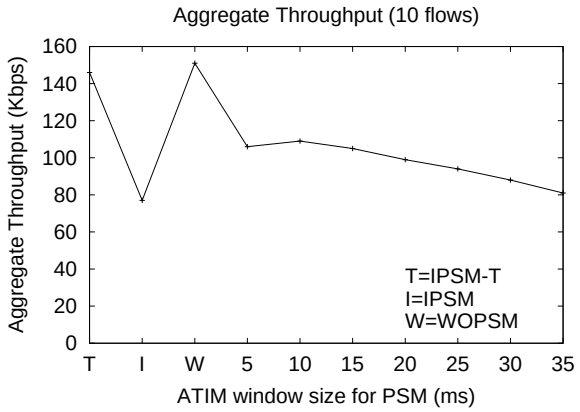

(a) Aggregate throughput (10 flows)

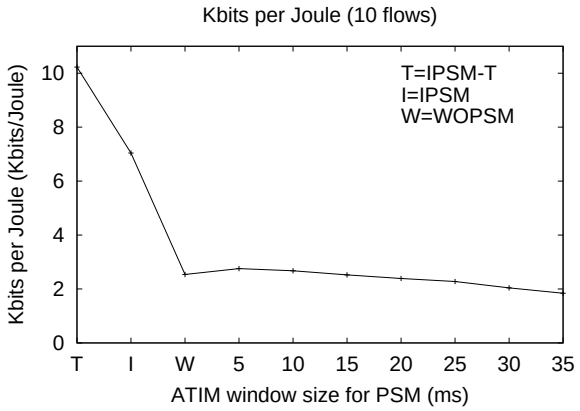

(b) Total data delivered per joule (10 flows)

Fig. 15. Random topology: 50 nodes with 10 tcp flows

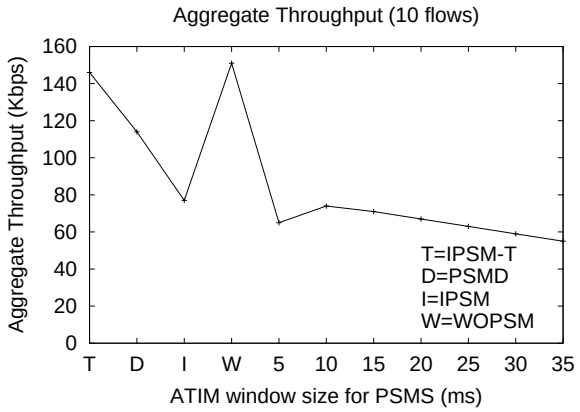

(a) Aggregate throughput (10 flows)

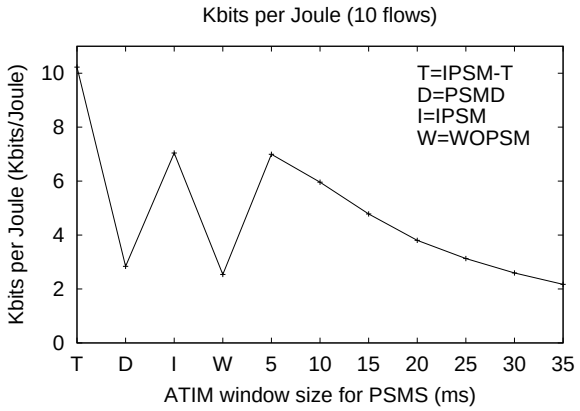

(b) Total data delivered per joule (10 flows)

Fig. 16. Random topology: 50 nodes with 10 tcp flows (PSMS)

use extra channel bandwidth for the ATIM window, which delays a sender to receive acknowledgments. This makes the congestion window increase slowly, which causes the TCP throughput degradation. For IPSM, nodes power off in the middle of beacon interval once they complete packet transmissions that are announced during the ATIM window. This causes a delay for a sender to receive acknowledgments. Therefore, IPSM performs worse than PSM. IPSM-T achieves the aggregate throughput that is comparable to that of WOPSM. Since we use on-off traffic, when there is no traffic, IPSM-T will use power saving mode. Thus, IPSM-T conserves energy much more than IPSM or PSM in Fig. 15 (b).

Since PSMS also allows for nodes to enter the doze state in the middle of beacon interval, the aggregate throughput for PSMS is also poor in Fig. 16 (a). The aggregate throughput of PSMD is little better than IPSM because in PSMD nodes stay awake for the entire beacon interval. In Fig. 16 (b), both PSMD and PSMS show some energy savings because of low throughput shown in Fig. 16 (a). IPSM-T yields the best energy savings among all schemes.

E. Summary

In this chapter, we have presented an energy efficient protocol that improves PSM for DCF in an IBSS of IEEE 802.11. The ATIM window size is fixed in PSM, which is a significant factor for both throughput and energy consumption. As the number of nodes increases or the network load gets heavier, the desirable ATIM window size becomes larger. Thus, a fixed ATIM window cannot perform very well all the time. In PSM, if the ATIM window is too small, the throughput degrades as the network load becomes heavier. If the ATIM window is too large, the energy gain from power saving mode becomes smaller since each node must stay awake during the ATIM window.

IPSM is based on PSM, but a node can dynamically adapt its ATIM window size

based on observed network conditions, which leads to a throughput comparable to that of IEEE 802.11 without power saving mode. In IPSM, a node also can power off its wireless network interface whenever it finishes packet transmission for the announced packets. This gives significant energy savings. Simulation results show that IPSM outperforms PSM with respect to energy savings.

We observe that the power saving mode does not work well with TCP traffic. When using the power saving mode nodes have to use extra channel bandwidth for the ATIM window, which delays a sender to receive acknowledgments. This makes the congestion window increase slowly, which causes the TCP throughput degradation. In order to improve TCP performance, nodes can temporarily give up the power saving mode when there exists TCP traffic in the network. Simulation results show this modification helps achieve a comparable throughput to IEEE 802.11 without the power saving mode and conserves energy more than IPSM or PSM.

CHAPTER III

POWER CONTROL *

Power control is a mechanism that varies a transmission power level when sending packets [26]. The primary benefit of power control is to increase channel capacity by reducing interferences among network nodes. The secondary benefit is to conserve energy by utilizing only necessary transmission power for packet transmissions.

A simple power control protocol has been proposed based on an RTS-CTS handshake in the context of IEEE 802.11 [1, 18, 28, 40]. Different power levels among different nodes introduce asymmetric links. Therefore, in the above scheme, RTS and CTS are transmitted using the highest power level and DATA and ACK are transmitted using the minimum power level necessary for the nodes to communicate. In this chapter, we show that this scheme has a shortcoming, which increases collisions and degrades network throughput. We present a new power control protocol which does not degrade throughput.

The rest of this chapter is organized as follows. Section A reviews the related work. Background on IEEE 802.11 is given in Section B. Section C describes a previously proposed power control scheme and its shortcoming. Section D presents our proposed power control MAC protocol. We will refer to the proposed scheme as PCM (Power Control MAC). Section E discusses simulation results. Section F summarizes this chapter.

A. Related Work

A power control mechanism that can be incorporated into the IEEE 802.11 RTS-CTS handshake is proposed in [28, 40]. The scheme in [40] allows a node, A, to specify its current transmission power level in the transmitted RTS, and allows receiver node B to include a desired transmission power level in the CTS sent back to A. On receiving the CTS, node A then transmits DATA using the power level specified in the CTS. This scheme allows B to help A choose the appropriate power level, so as to maintain a desired signal-to-noise ratio. A similar protocol is utilized in [18], wherein the RTS and CTS packets are sent at the highest power level, and the DATA and ACK may be sent at a lower power level. We refer to this scheme as the *BASIC* power control MAC protocol. We found that the BASIC scheme has a shortcoming that can degrade the throughput. Furthermore, the BASIC scheme may potentially increase the energy consumption, instead of decreasing it. We elaborate on this in Section 2.

PARO [18], a power-aware routing optimization, determines routes which consume low energy. PARO chooses a cost function based on the transmission power level at each hop on a route, to determine a low energy-consuming route between a pair of nodes. PARO also uses a power control MAC protocol similar to BASIC. Several other routing metrics are also proposed in [47, 50].

A power control protocol presented in [1] is also similar to the BASIC scheme. It maintains a table for the minimum transmission power necessary to communicate with neighbor nodes. This scheme allows each node to increase or decrease its power level dynamically. However, different power levels among nodes result in asymmetric links, causing collisions.

A power control protocol proposed in [56] uses one control channel and multiple data channels. A control channel is used to assign data channels to nodes. An RTS, CTS, RES

(a special packet), and broadcast packets are transmitted through the control channel using the highest transmission power. By an RTS-CTS handshake, source and destination nodes decide which channel and what power level to use for data transmissions. On the reception of CTS, the source sends an RES to the destination to reserve a data channel. Then, DATA and ACK transmissions occur on the reserved data channel using the negotiated power level from the RTS-CTS handshake.

Transmit power is controlled according to packet size in [13, 14]. The proposed scheme is based on the observation that reducing transmission power can result in energy savings, but can also result in more errors. A higher bit error rate can lead to increased retransmissions, consuming more energy. Thus, the protocol in [13, 14] chooses an appropriate transmission power level based on the packet size. An adaptive scheme is also presented in [31] to choose MAC frame size based on the channel conditions.

IEEE 802.11 may result in unfairness (performance degradation) for nodes which use lower transmission power than their neighbor nodes. Poojary *et al.* [39] propose a scheme to improve the fairness.

COMPOW [38] selects a common power level at all nodes in the network to ensure bi-directional links. Each node runs several routing daemons, each at a different power level. The power level is chosen to be the smallest power level which achieves the same level of network connectivity as the highest power level.

The Power Controlled Multiple Access (PCMA) protocol [37] allows different nodes to have different transmission power levels (and allows per-packet selection of transmission power). PCMA uses two channels, one channel for “busy tones”, and the other for all other packets. PCMA uses busy tones, instead of RTS-CTS, to overcome the hidden terminal problem. While a node is receiving a DATA packet, it periodically sends a busy tone. The power level at which the busy tone is transmitted by a node is equal to the maximum additional noise the node can tolerate. Any node wishing to transmit a packet first waits

for a fixed duration (determined by the frequency with which nodes transmit busy tones when receiving data), and senses the channel for busy tones from other nodes. The signal strength of busy tones received by a node is utilized to determine the highest power level at which this node may transmit without interfering with other on-going transmissions. Busy tones with two separate channels are also used in [11, 20, 47, 57].

In [41, 42, 43, 52], power control is used for the purpose of topology control. Power control has been also used to establish energy efficient spanning trees for multicasting and broadcasting [53, 54].

B. IEEE 802.11 MAC Protocol

IEEE 802.11 specifies two medium access control protocols, PCF (Point Coordination Function) and DCF (Distributed Coordination Function). PCF is a centralized scheme, whereas DCF is a fully distributed scheme. We consider DCF in this dissertation.

We now define the terms *transmission range, carrier sensing range* and *carrier sensing zone* which are used in the rest of the chapter:

- *Transmission range*: When a node is within transmission range of a sender node, it can receive and correctly decode packets from the sender node. In our simulations, the transmission range is 250 m when using the highest transmission power level.
- *Carrier sensing range*: Nodes in the carrier sensing range can sense the sender's transmission. Carrier sensing range is typically larger than the transmission range, for instance, two times larger than the transmission range [27]. In our simulations, the carrier sensing range is 550 m when using the highest power level. Note that the carrier sensing range and transmission range depend on the transmission power level. Since carrier sensing range includes the transmission range, we now define *carrier sensing zone* which excludes the transmission range from the carrier sensing range.

- *Carrier sensing zone*: When a node is within the carrier sensing zone, it can sense the signal but cannot decode it correctly. Note that, as per our definition here, the carrier sensing zone does not include transmission range. Nodes in the transmission range can indeed sense the transmission, but they can also decode it correctly. Therefore, these nodes will not be in the carrier sensing zone as per our definition. The carrier sensing zone is between 250 m and 550 m with the highest power level in our simulation.

Fig. 17 shows the transmission range, carrier sensing range, and carrier sensing zone for node C[1]. When node C transmits a packet, B and D can receive and decode it correctly since they are in transmission range. However, A and E only sense the signal and cannot decode it correctly because they are in the carrier sensing zone.

The DCF in IEEE 802.11 is based on CSMA/CA (Carrier Sense Multiple Access with Collision Avoidance). Carrier sensing is performed using physical carrier sensing (by air interface) as well as virtual carrier sensing. Virtual carrier sensing uses the duration of the packet transmission, which is included in the header of RTS, CTS, and DATA frames. The duration included in each of these frames can be used to infer the time when the source node would receive an ACK frame from the destination node. For example, the duration field in RTS includes time for CTS, DATA, and ACK transmissions. Similarly, the duration field for CTS includes time for DATA and ACK transmissions, and the duration field for DATA only includes time for the ACK transmission.

Each node in IEEE 802.11 maintains a NAV (Network Allocation Vector) which indicates the remaining time of the on-going transmission sessions. Using the duration information in RTS, CTS, and DATA packets, nodes update their NAVs whenever they receive a packet. The channel is considered to be busy if either physical or virtual carrier sensing

[1]Transmission range and carrier sensing range may not be circular in reality.

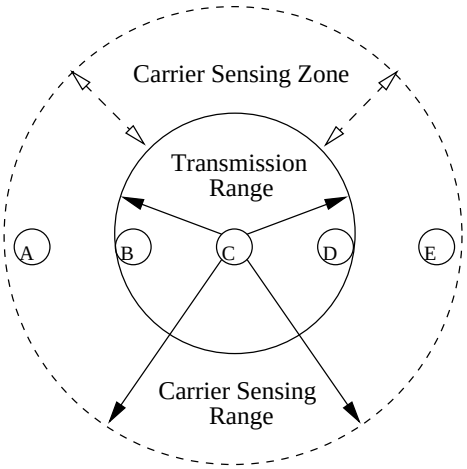

Fig. 17. Nodes in transmission range can receive and decode packet correctly, whereas nodes in the carrier sensing zone can sense a transmission, but cannot decode it correctly.

indicates that the channel is busy.

Fig. 18 shows how nodes in transmission range and the carrier sensing zone adjust their NAVs during RTS-CTS-DATA-ACK transmission. SIFS, DIFS, and EIFS are interframe spaces (IFSs) specified in IEEE 802.11. Note that in Fig. 18 the lengths of RTS, CTS, DATA, and ACK do not exactly represent the actual sizes.

IFS is the time interval between frames. IEEE 802.11 defines four IFSs – SIFS (short interframe space), PIFS (PCF interframe space), DIFS (DCF interframe space), and EIFS (extended interframe space). The IFSs provide priority levels for accessing the channel. The SIFS is the shortest of the interframe spaces and is used after RTS, CTS, and DATA frames to give the highest priority to CTS, DATA and ACK, respectively. In DCF, when the channel is idle, a node waits for the DIFS duration before transmitting any packet.

In Fig. 18, nodes in transmission range correctly set their NAVs when receiving RTS or CTS. However, since nodes in the carrier sensing zone cannot decode the packet, they do not know the duration of the packet transmission. To prevent a collision with the ACK reception at the source node, when nodes detect a transmission and cannot decode it, they

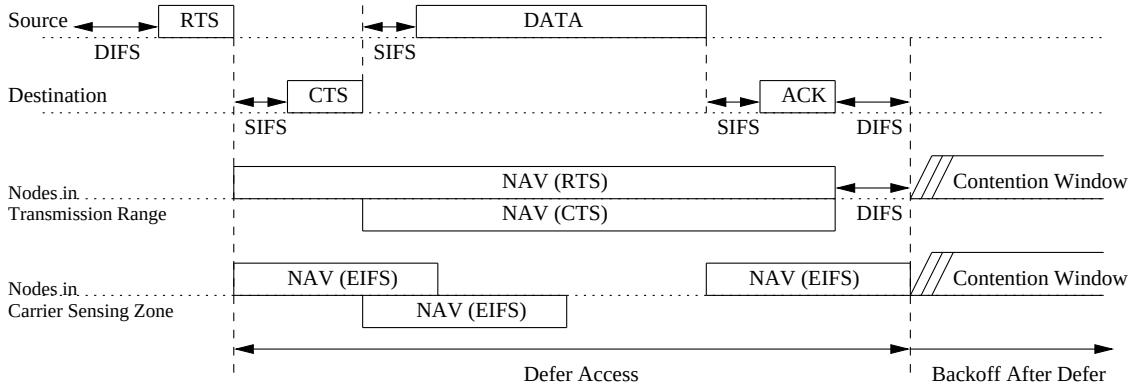

Fig. 18. When source and destination nodes transmit RTS and CTS, nodes in transmission range correctly receive these packets and set their NAVs for the duration of the whole packet transmission. However, nodes in the carrier sensing zone only sense the signal and cannot decode it correctly, so these nodes set their NAVs for EIFS duration (when they sense the channel changing state from busy to idle). The purpose of EIFS is to protect an ACK frame at the source node.

set their NAVs for the EIFS duration. The main purpose of the EIFS is to provide enough time for a source node to receive the ACK frame, so the duration of EIFS is longer than that of an ACK transmission. As per IEEE 802.11, the EIFS is obtained using the SIFS, the DIFS, and the length of time to transmit an ACK frame at the physical layer's lowest mandatory rate, as the following equation [23]: $EIFS = SIFS + DIFS + [(8 \times ACKsize) + PreambleLength + PLCPHeaderLength]/BitRate$, where ACK size is the length (in bytes) of an ACK frame, and BitRate is the physical layer's lowest mandatory rate. PreambleLength is 144 bits and PLCPHeaderLength is 48 bits [23]. Using a 1 Mbps channel bit rate, EIFS is equal to 364 μs.

In IEEE 802.11 [23], the EIFS is used whenever the physical layer has indicated to the MAC that a frame transmission was begun but that frame transmission did not result in the correct reception of a complete MAC frame with a correct FCS (Frame Check Sequence) value. (In this context, a frame transmission is considered to have begun when its PLCP

header is received correctly.) The EIFS interval begins following indication by the physical layer that the channel is idle after sensing of the erroneous frame. In our simulations, we use a somewhat conservative variation on the above 802.11 specification. In our simulation model of the 802.11 protocol, whenever a node senses a transmission (whether or not PLCP header is received) but cannot receive the transmission correctly, EIFS is used. Thus, nodes in the carrier sensing zone use EIFS whenever they can sense the signal but cannot decode it. In the rest of this chapter (and Fig. 18), unless otherwise mentioned, when we say 802.11, we refer to the above conservative variation. This variation may reduce collisions as compared to the IEEE 802.11 standard in multi-hop wireless networks.

Note that IEEE 802.11 does not completely prevent collisions due to a hidden terminal – nodes in the receiver's carrier sensing zone, but not in the sender's carrier sensing zone or transmission range, can cause a collision with the reception of a DATA packet at the receiver. For example, in Fig. 19, suppose node C transmits a packet to node D. When C and D transmit an RTS and CTS respectively, nodes A and F will set their NAVs for EIFS duration. During C's DATA transmission, A defers its transmission because it senses C's DATA transmission. However, node F does not sense any signal during C's DATA transmission, so it considers the channel to be idle. (F is in D's carrier sensing zone, but not in C's.) When F starts a new transmission, it can cause a collision with the reception of DATA at D. As F is outside D's transmission range, by symmetry, D may be outside F's transmission range. However, since F is in D's carrier sensing zone, by symmetry, this implies that F can present sufficient interference at node D to cause a collision with DATA being received by D.

C. BASIC Power Control Protocol

This section describes the BASIC power control scheme [1, 18, 28, 40] and its limitation.

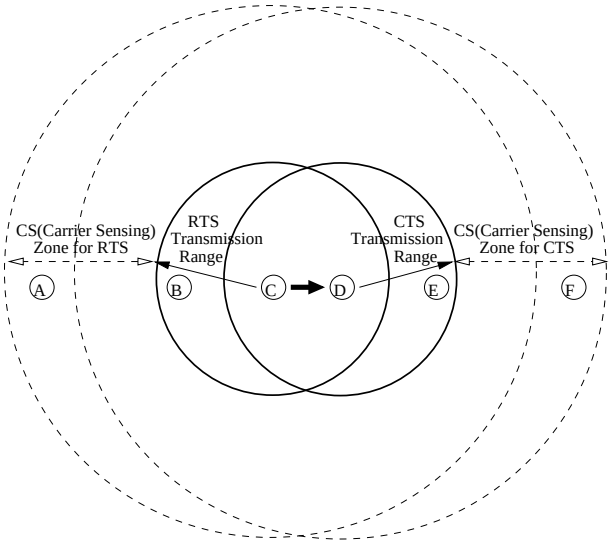

Fig. 19. IEEE 802.11 does not prevent collisions completely. After the RTS-CTS handshake, when node C transmits a DATA packet to node D, F cannot sense the DATA transmission since it is in D's carrier sensing zone but not C's. Therefore, when F starts transmitting, it can cause a collision with the reception of the DATA packet at node D.

1. Protocol Description

As mentioned earlier, power control can reduce energy consumption. However, power control may introduce different transmission power levels at different hosts, creating an asymmetric situation where a node A can reach node B, but B cannot reach A.

Different transmission powers used at different nodes may also result in increased collisions, unless some precautions are taken. Suppose nodes A and B in Fig. 20 use lower power than nodes C and D. When A is transmitting a packet to B, this transmission may not be sensed by C and D. So, when C and D transmit to each other using a higher power, their transmissions will collide with the on-going transmission from A to B.

One simple solution (as a modification to IEEE 802.11) is to transmit RTS and CTS at the highest possible power level but transmit DATA and ACK at the minimum power level necessary to communicate, as suggested in [1, 18, 28, 40]. We refer to this as the BASIC

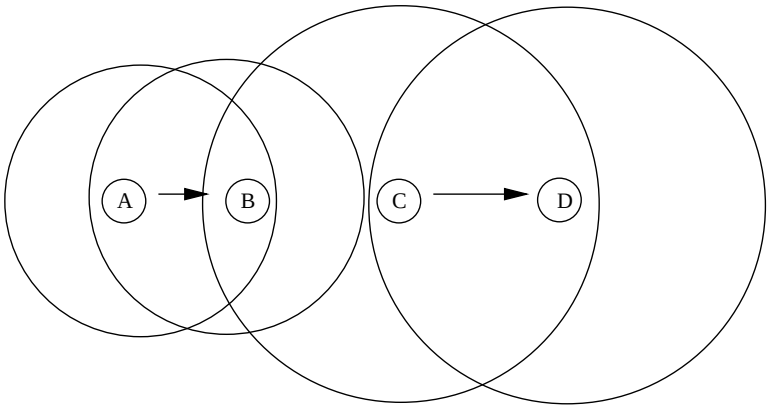

Fig. 20. Differences in transmission power can lead to increased collisions.

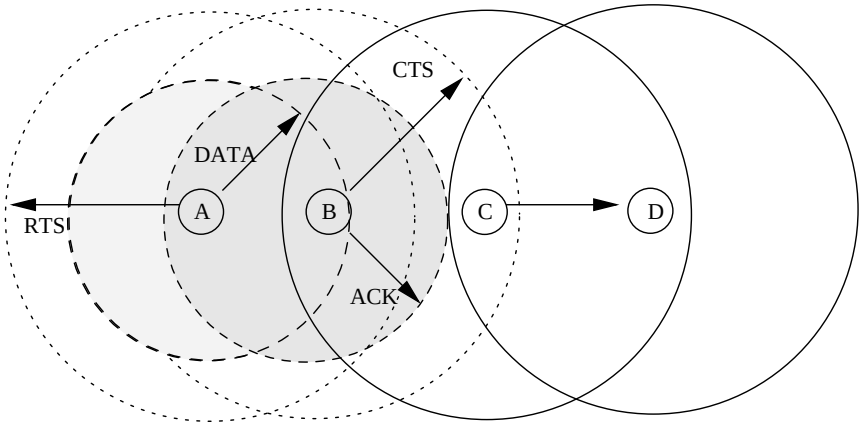

Fig. 21. BASIC scheme: RTS and CTS are transmitted at the highest transmission power level.

scheme. Fig. 21 illustrates the BASIC scheme. In Fig. 21, nodes A and B send RTS and CTS, respectively, with the highest power level so that node C receives the CTS and defers its transmission. By using a lower power for DATA and ACK packets, nodes can conserve energy.

In the BASIC scheme, the RTS-CTS handshake is used to decide the transmission power for subsequent DATA and ACK packets. This can be done in two different ways as described below. Let p_{max} denote the maximum possible transmission power level:

- Suppose that node A wants to send a packet to node B. Node A transmits the RTS at power level p_{max}. When B receives the RTS from A with signal level p_r, B can calculate the minimum necessary transmission power level, $p_{desired}$, for the DATA packet based on received power level p_r, the transmitted power level, p_{max}, and noise level at the receiver B. We can borrow the procedure for estimating $p_{desired}$ from [37]. This procedure determines $p_{desired}$ taking into account the current noise level at node B. Node B then specifies $p_{desired}$ in its CTS to node A. After receiving CTS, node A sends DATA using power level $p_{desired}$. Since the signal-to-noise ratio at the receiver B is taken into consideration, this method can be accurate in estimating the appropriate transmission power level for DATA.

- In the second alternative, when a destination node receives an RTS, it responds by sending a CTS as usual (at power level p_{max}). When the source node receives the CTS, it calculates $p_{desired}$ based on received power level, p_r, and transmitted power level (p_{max}), as

$$p_{desired} = \frac{p_{max}}{p_r} \times Rx_{thresh} \times c$$

where Rx_{thresh} is the minimum necessary received signal strength and c is a constant (similar to [37]). We set c equal to 1 in our simulations. Then, the source transmits DATA using a power level equal to $p_{desired}$. Similarly, the transmission power for the

ACK transmission is determined when the destination receives the RTS.

This method makes two assumptions. First, signal attenuation between source and destination nodes is assumed to be the same in both directions. Second, noise level at the receiver is assumed to be below some predefined threshold. This approach may result in unreliable communication when the assumptions are wrong. However, it is likely to be reliable with a fairly high probability. This alternative does not require any modification to the CTS format. We use this alternative in our simulation of BASIC and the proposed scheme.

As we now explain below, the BASIC scheme can lead to increased collisions, degrading throughput.

2. Deficiency of the BASIC Protocol

In the BASIC scheme, RTS and CTS are sent using p_{max}, and DATA and ACK packets are sent using the minimum necessary power to reach the destination. When the neighbor nodes receive an RTS or CTS, they set their NAVs for the duration of the DATA-ACK transmission. For example, in Fig. 22, suppose node D wants to transmit a packet to node E. When D and E transmit the RTS and CTS respectively, B and C receive the RTS, and F and G receive the CTS, so these nodes will defer their transmissions for the duration of the D-E transmission. Node A is in the carrier sensing zone of D (when D transmits at p_{max}) so it will only sense the signals and cannot decode the packets correctly. Node A will set its NAV for EIFS duration when it senses the RTS transmission from D. Similarly, node H will set its NAV for EIFS duration following CTS transmission from E.

When transmission power control is not used, the carrier sensing zone is the same for RTS-CTS and DATA-ACK since all packets are sent using the same power level. However, in BASIC, when a source and destination pair decides to reduce the transmission power

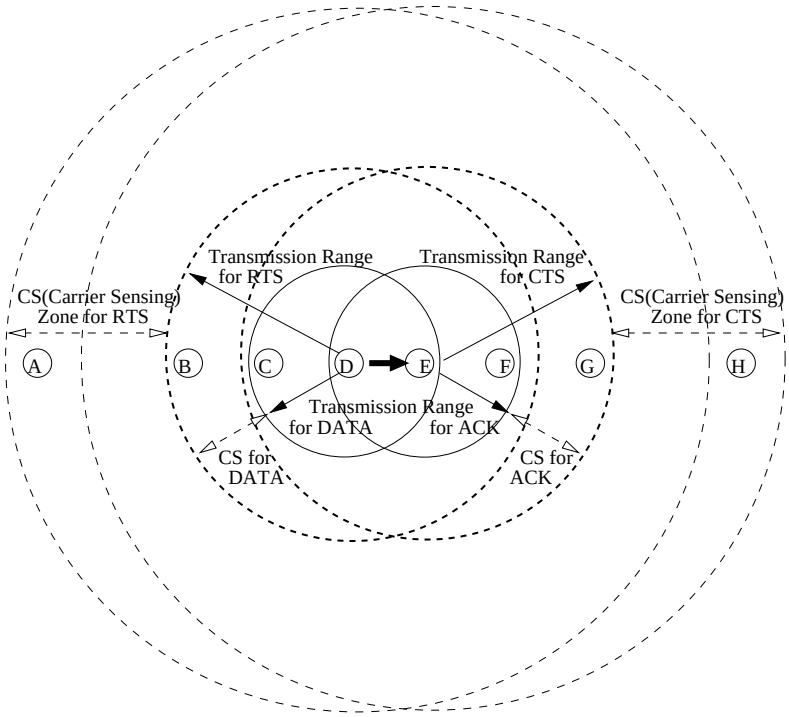

Fig. 22. BASIC scheme: Suppose node D transmits a packet to node E. Since DATA and ACK are transmitted using the minimum necessary transmission power, nodes in carrier sensing zone (such as A and H) during the RTS-CTS transmission may not sense any signal during DATA-ACK. When these nodes initiate a new transmission by sending RTS at the power level p_{max}, a collision may occur at D and E. The collisions trigger retransmissions, resulting in more energy consumption.

for DATA-ACK, the transmission range for DATA-ACK is smaller than that of RTS-CTS; similarly, the carrier sensing zone for DATA-ACK is also smaller than that of RTS-CTS.

When D and E in Fig. 22 reduce their transmission power for DATA and ACK transmissions respectively, both transmission range and carrier sensing zone are reduced. Thus, only C and F can correctly receive the DATA and ACK packets, respectively. Furthermore, since nodes A and H cannot sense the transmissions, they consider the channel to be idle. When any of these nodes (A or H) starts transmitting at the power level p_{max}, this transmission causes a collision with the ACK packet at D and DATA packet at E. This results in throughput degradation and higher energy consumption (because of retransmissions), as we will see in Section 3.

As discussed in Section B, IEEE 802.11 also does not prevent nodes in the carrier sensing zone (node H in Fig. 22) from causing collisions with the DATA packet at the destination node (node E in Fig. 22). However, BASIC makes the situation worse by introducing interference with the reception of an ACK at the source node. Using BASIC, node A in Fig. 22 cannot sense D's DATA transmission at the lower power level, so a transmission from A can interfere with the reception of the ACK at D.

The above discussion indicates that the BASIC scheme is more prone to collisions, degrading throughput (as shown in Section 3). The BASIC scheme has been considered for saving energy [1, 18, 28, 40]. However, past work did not identify the above deficiency of the BASIC protocol. For instance, reference [18] considers 100 x 100 m^2 area for the simulation. In this case, every node can correctly decode the RTS or CTS and will know the duration of the remaining packet transmission. In such an environment, the negative impact of BASIC power control is not manifested.

D. Proposed Power Control MAC Protocol

Proposed Power Control MAC (PCM) is similar to the BASIC scheme in that it uses power level p_{max} for RTS-CTS and the minimum necessary transmission power for DATA-ACK transmissions. We now describe the procedure used in PCM:

1. Source and destination nodes transmit the RTS and CTS using p_{max}. Nodes in the carrier sensing zone set their NAVs for EIFS duration when they sense the signal and cannot decode it correctly (similar to the variation on IEEE 802.11 described earlier).
2. The source node may transmit DATA using a lower power level, similar to the BASIC scheme.
3. To avoid a potential collision with the ACK (as discussed earlier), the source node transmits DATA at the power level p_{max}, periodically, for just enough time so that nodes in the carrier sensing zone can sense it.
4. The destination node transmits an ACK using the minimum required power to reach the source node, similar to the BASIC scheme.

Fig. 23 shows how the transmission power level changes during the sequence of an RTS-CTS-DATA-ACK transmission. After the RTS-CTS handshake using p_{max}, suppose the source and destination nodes decide to use power level p_1 for DATA and ACK. Then, the source will transmit DATA using p_1 and periodically use p_{max}. The destination uses p_1 for ACK transmission.

As we described, the key difference between PCM and the BASIC scheme is that PCM periodically increases the transmission power to p_{max} during the DATA packet transmission. With this change, nodes that can potentially interfere with the reception of ACK at the sender will periodically sense the channel as busy, and defer their own transmission. Since nodes that can sense a transmission but not decode it correctly only defer for EIFS

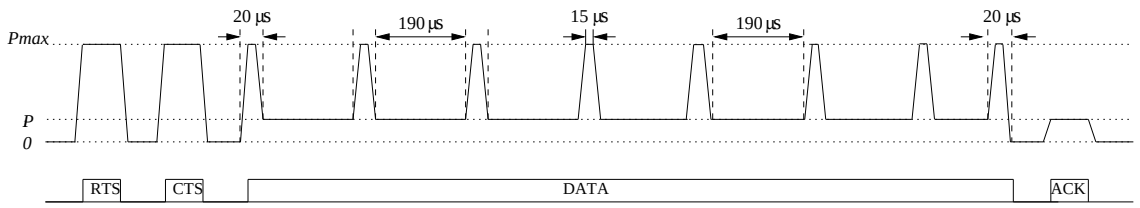

Fig. 23. PCM periodically increases the transmission power during DATA transmission in order to inform nodes in the carrier sensing zone of its transmission.

duration, the transmission power for DATA is increased once every EIFS duration. Also, the interval which the DATA is transmitted at p_{max} should be larger than the time required for physical carrier sensing.

According to [23], 15 μs should be adequate for carrier sensing, and time required to increase output power (power-on) from 10% to 90% of maximum power (or power-down from 90% to 10% of maximum power) should be less than 2 μs. Thus, we believe 20 μs should be enough to power up (2 μs), sense the signal (15 μs), and power down (2 μs).

In our simulation, EIFS duration is set to 212 μs using a 2 Mbps bit rate[2]. In PCM, a node transmits DATA at p_{max} every 190 μs for a 20 μs duration. Thus, the interval between the transmissions at p_{max} is 210 μs, which is shorter than EIFS duration. A source node starts transmitting DATA at p_{max} for 20 μs and reduces the transmission power to a power level adequate for the given transmission for 190 μs. Then, it repeats this process during DATA transmission, (see Fig. 23). The node also transmits DATA at p_{max} for the last 20 μs of the transmission.

With the above simple modification, PCM overcomes the problem of the BASIC scheme and can achieve throughput comparable to 802.11, but uses less energy. However,

[2]According to the 802.11 standard [23], EIFS is equal to 364 μs when the lowest data rate is 1 Mbps. In our simulation, we use 2 Mbps bit rate as the lowest data rate, so EIFS is equal to 212 μs. Note that the performance of PCM will improve if we use 364 μs for EIFS because PCM will increase the transmission power level less frequently.

note that PCM, just like 802.11, does not prevent collisions completely. Specifically, collisions with DATA being received by the destination can occur, as discussed earlier. Our goal in this chapter is to match the performance of 802.11 while reducing energy consumption.

To be more conservative in estimating the energy consumption of PCM, we also perform our simulations where we increase the transmission power every 170 μs for 40 μs during DATA transmission. We refer to this variation as PCM40. This variation will consume more energy as compared to the above version of PCM.

Recall that, as discussed earlier, we evaluates a variation of IEEE 802.11 wherein EIFS is used differently from the standard. However, the proposed approach of transmitting part of a packet at a higher power level and rest at (potentially) lower power level can be applied to the IEEE 802.11 specification as well. For instance, when the rate at which the data is transmitted is greater than the rate used for PLCP header, the range over which PLCP header is received can be greater than the range over which data is received. We can exploit this by transmitting the PLCP header at p_{max} and the rest of the packet at the lower power level. This is expected to eliminate some collisions, but perhaps not all the collisions introduced by the BASIC scheme. This dissertation, however, only evaluates the variation of 802.11, and the PCM scheme.

E. Performance Evaluation

We simulate BASIC, PCM, PCM40, as well as 802.11. We use the following two metrics to evaluate the MAC protocols:

- *Aggregate throughput over all flows in the network.*
- *Total data delivered per unit of transmission energy consumption (or, Mbits delivered per joule)*: This is calculated as the total data delivered by all the flows divided by the total amount of *transmission* energy consumption over all nodes (Mbits/joule).

The energy consumed in packet reception is not counted in the above metric.

1. Simulation Model

For simulations, we use ns-2 with the CMU wireless extension [10]. We use 2 Mbps for the channel bit rate. Packet size is 512 bytes unless otherwise specified. (We perform some simulations varying packet sizes as well.) Each flow in the network transmits CBR (Constant Bit Rate) traffic. We perform the simulation with various network loads. We do not consider mobility in our simulations.

For the radio propagation model, a two-ray path loss model is used [10]. The transmitted signal is attenuated by $\frac{1}{d^2}$ at near distances and by $\frac{1}{d^4}$ at far distances, where d is the distance between the source and the destination nodes. We do not consider fading in our simulations.

We assume that carrier sensing range is about two times larger than the transmission range. In particular, in our simulation, the transmission range is 250 m, and the carrier sensing range is 550 m, at the highest transmission power level. All simulation results are the average of 30 runs. Each simulation runs for 20 seconds of simulation time.

2. Simulation Topology

For network topologies, we use both a simple chain and random topologies.

For the chain topology, we consider 10 transmission power levels, 1 mW, 2 mW, 3.45 mW, 4.8 mW, 7.25 mW, 10.6 mW, 15 mW, 36.6 mW, 75.8 mW, and 281.8 mW, which roughly correspond to the transmission ranges of 40 m, 60 m, 80 m, 90 m, 100 m, 110 m, 120 m, 150 m, 180 m, and 250 m, respectively. For the random topology, we consider four transmission power levels, 2 mW, 15 mW, 75.8 mW, and 281.8 mW, roughly corresponding to the transmission ranges of 60 m, 120 m, 180 m, and 250 m, respectively. Since the simulation results for the BASIC scheme show dramatic changes as the node distances varies,

we include more transmission power levels for the chain topology in order to understand the behavior of the BASIC scheme. The transmission range at power level p_{max} is 250 m in our simulations for both topologies:

- *Chain topology*

  Fig. 24 shows our chain topology, which consists of 31 nodes with 30 single hop flows. Nodes are shown as a circle, and the arrow between two nodes indicates traffic flows. The distance between adjacent node pairs in Fig. 24 is uniform. In our simulations, we vary the distance from 40 m to 250 m.

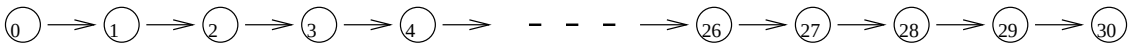

Fig. 24. Chain topology: 31 nodes with 30 flows.

- *Random topology: one hop flows*

  For the random topology, we place 50 nodes randomly within a 1000x1000 m^2 flat area. One flow originates at each node with the nearest node as its destination. Thus, a total of 50 flows are generated. We simulate 50 different random topologies (scenarios). Table I shows the number of flows using each power level for each scenario. In Table I, p_1, p_2, p_3, and p_4 indicate transmission power levels, corresponding to the transmission ranges of 60 m, 120 m, 180 m, and 250 m, respectively.

- *Random topology: multi-hop flows*

  We also simulate the random topology with multi-hop flows. In a 1000x1000 m^2 flat area, 100 nodes are randomly placed. For the traffic, 60 nodes are randomly chosen (30 sources and 30 destinations) among 100 nodes – total 30 flows are generated. The average path length of the generated flows is 6 hops with a range of 1 to 15 hops. Fifty different scenarios are simulated for multi-hop topologies.

Table I. Number of Flows at Various Power Levels for the Random Topology

Scenario	1	2	3	4	5	6	7	8	9	10	11	12	13	14	15	16	17	18	19	20	21	22	23	24	25
p1 flows	15	14	10	18	11	16	16	15	17	17	18	5	14	12	10	19	8	11	7	13	12	13	6	12	12
p2 flows	18	23	28	23	26	17	24	24	22	24	18	27	27	24	23	16	27	27	27	25	27	21	27	26	19
p3 flows	14	10	9	8	9	14	10	10	8	8	11	13	8	12	15	13	13	9	13	6	8	14	15	9	16
p4 flows	3	3	3	1	4	3	0	1	3	1	3	5	1	2	2	2	2	3	3	6	3	2	2	3	3
Total	50	50	50	50	50	50	50	50	50	50	50	50	50	50	50	50	50	50	50	50	50	50	50	50	50

Scenario	26	27	28	29	30	31	32	33	34	35	36	37	38	39	40	41	42	43	44	45	46	47	48	49	50
p1 flows	18	18	13	15	16	8	14	13	20	16	15	11	15	15	11	16	17	12	12	7	7	15	14	17	11
p2 flows	16	19	20	26	18	25	22	20	17	17	20	25	17	18	22	18	17	24	22	31	25	17	21	24	25
p3 flows	11	10	13	8	11	12	8	13	12	15	12	12	16	12	14	13	11	12	15	10	15	16	15	6	12
p4 flows	5	3	4	1	5	5	6	4	1	2	3	2	2	5	3	3	5	2	1	2	3	2	0	3	2
Total	50	50	50	50	50	50	50	50	50	50	50	50	50	50	50	50	50	50	50	50	50	50	50	50	50

3. Simulation Results

We first discuss the simulation results for the chain topology. We consider the random topology later.

a. Chain Topology: Varying Node Distance

Fig. 25 shows the simulation results for 31 nodes with 30 flows in a chain topology. Each flow generates traffic at the rate of 1 Mbps. Recall that PCM is our proposed scheme where transmission power is increased to p_{max} every 190 μs for 20 μs, and PCM40 is a variation of PCM where the transmission power is increased to p_{max} every 170 μs for 40 μs during DATA transmission.

As the distance between two neighbors increases in Fig. 25 (a), the aggregate throughput of all schemes increases. This is because when nodes are far apart, a larger number of nodes can transmit simultaneously.

PCM, PCM40 and 802.11 achieve comparable aggregate throughput as seen from the overlapping curves in Fig. 25 (a), but the BASIC scheme performs poorly in most cases. To understand the graph, we use Table II, which shows the number of nodes in the carrier

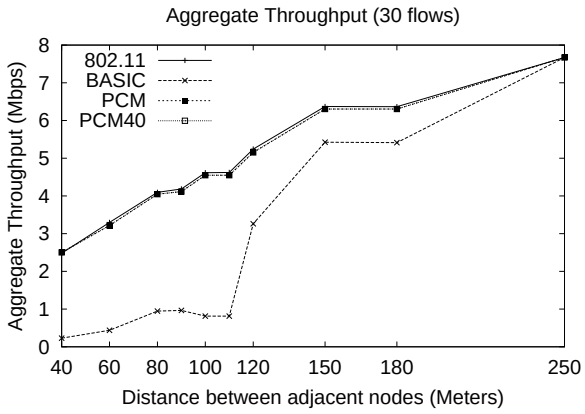

(a) Aggregate throughput

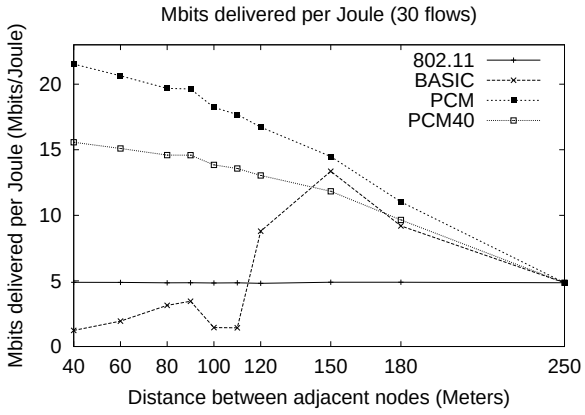

(b) Total data delivered per joule

Fig. 25. Chain topology: Each flow generates traffic at a rate of 1 Mbps: the curves for PCM, PCM40, and 802.11 overlap in (a).

Table II. BASIC – The Number of Nodes in the Carrier Sensing Zone

Distance (m)	40	60	80	90	100	110	120	150	180	250
Number of Interfering nodes	14	10	6	8	6	6	4	2	2	1

sensing zone. Table II shows the number of nodes that can interfere with a transmission between two neighbors at the center of the chain, that is, the transmission from node 14 to node 15 in Fig. 24. Thus the table shows the number of nodes which can interfere with DATA reception at receiver node 15 or ACK reception at sender node 14 in Fig. 24. The trend of the number of nodes in the carrier sensing zone shown in Table II is similar for other transmissions in the chain topology as well. Specifically, the number of nodes in the carrier sensing zone is decreasing (except at 90 m[3]) as the distance between nodes increases. This explains the graph in Fig. 25 (a); the aggregate throughput curve for the BASIC scheme in Fig. 25 (a) follows the same trend as that in Table II. As the number of potential collisions becomes smaller, the aggregate throughput increases in Fig. 25 (a). The aggregate throughput of the BASIC scheme jumps at the 120 m and 150 m points in Fig. 25 (a) mainly because of less collisions.

The total data delivered per joule with the BASIC scheme is worse than 802.11 for many cases in Fig. 25 (b). This is due to poor aggregate throughput with BASIC and extra energy consumption from collisions and retransmissions. Since PCM40 consumes more energy compared to PCM, it gives less data delivered per joule, but it still performs better than 802.11, or BASIC (except for the 150 m distance).

[3]The number of nodes in the carrier sensing range at p_{max} (550 m) is 12 for both 80 and 90 m distance networks. However, the number of nodes in the transmission range at p_{max} (250 m) for 80 and 90 m distance networks is 6 and 4, respectively. Therefore, the number of nodes in the carrier sensing zone for 80 and 90 m distance networks in Table II is 6 ($12 - 6 = 6$) and 8 ($12 - 4 = 8$), respectively.

When the adjacent nodes are 250 meters apart, BASIC and PCM cannot reduce the transmission power for DATA-ACK. (Recall that the transmission range at p_{max} is 250 m.) Therefore, in Fig. 25, all four schemes (802.11, BASIC, PCM and PCM40) perform the same when nodes are 250 m apart.

b. Chain Topology: Varying Network Load

Figs. 26 and 27 show the simulation results for 3 different node distances (60 m, 120 m, and 180 m) in the chain topology, with a varying data rate (load) per flow.

When the network is lightly loaded in Fig. 26 (a), the aggregate throughput of all the schemes is identical. Fig. 26 (a) also shows that the aggregate throughput of BASIC is much less than that of PCM and 802.11 at a moderate to high load. Simulation results for 120 m and 180 m distances in Fig. 26 (b) and (c) are similar to the 60 m distance in Fig. 26 (a). PCM, PCM40, and 802.11 curves overlap in Fig. 26.

Fig. 27 shows the total data delivered per joule for distances of 60 m, 120 m, and 180 m. It is interesting to see that the total data delivered per joule for PCM in Fig. 27 is higher than that of BASIC even when the aggregate throughput for both schemes is the same in Fig. 26. In PCM, nodes periodically increase the transmission power to p_{max}, which should cause higher energy consumption compared to BASIC. However, with BASIC more collisions occur, and when nodes retransmit packets, additional energy is consumed. Therefore, the net result is that BASIC consumes more energy than PCM.

Fig. 27 also indicates that as node distance increases, the total data delivered per joule for BASIC gets better. This is because as node distance increases, the number of collisions decreases (see Table II), hence the number of retransmissions decreases.

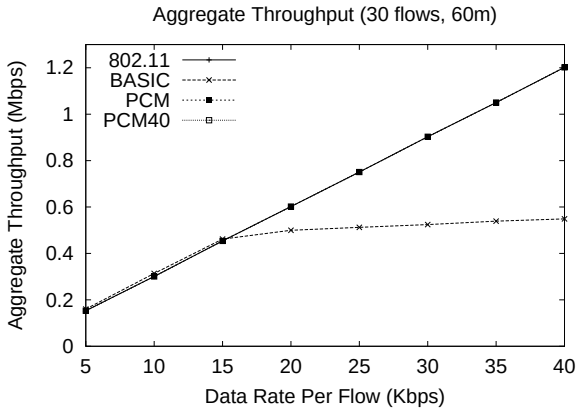

(a) Aggregate throughput (60 m Distance)

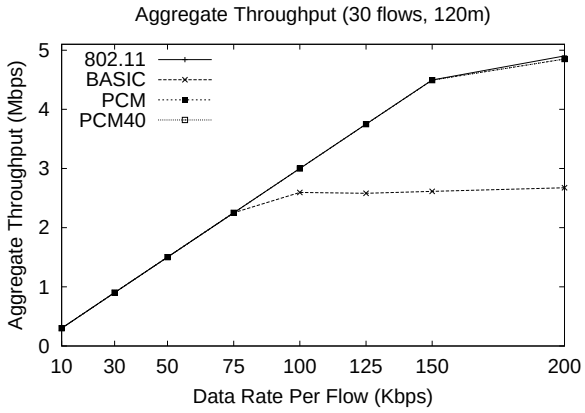

(b) Aggregate throughput (120 m Distance)

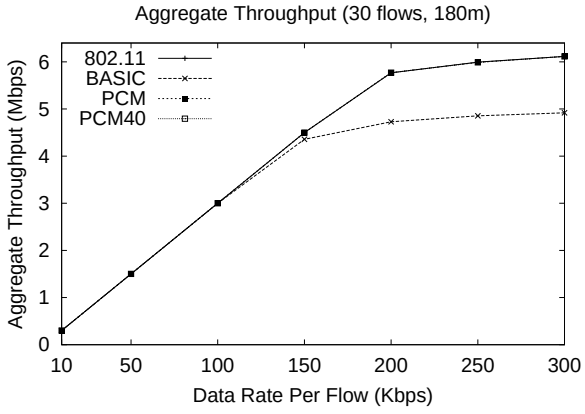

(c) Aggregate throughput (180 m Distance)

Fig. 26. Chain topology: As the network load increases, aggregate throughput for all four schemes also increases. However, the aggregate throughput of BASIC saturates sooner.

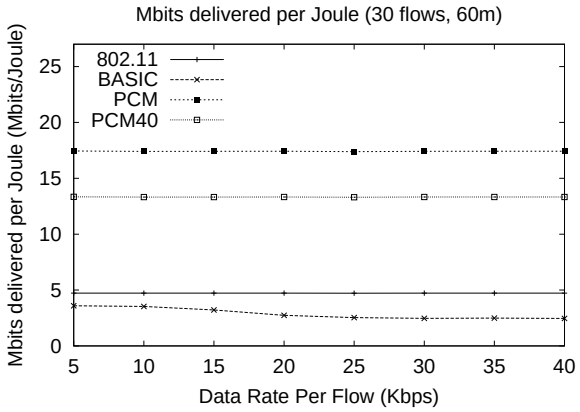

(a) Total data delivered per joule (60 m Distance)

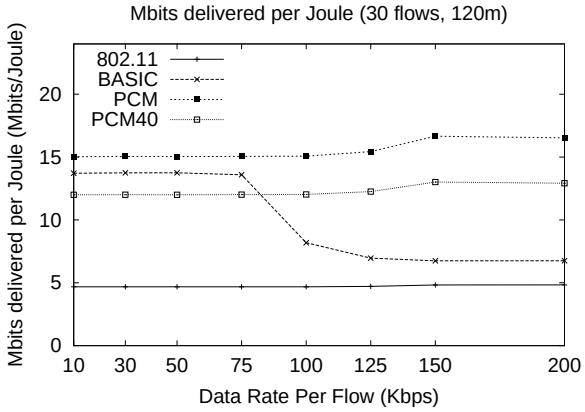

(b) Total data delivered per joule (120 m Distance)

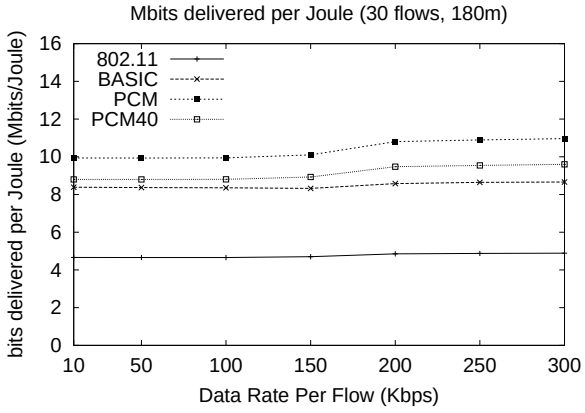

(c) Total data delivered per joule (180 m Distance)

Fig. 27. Chain topology: A large number of retransmissions in BASIC results in more energy consumption.

c. Random Topology: Varying Network Load (one hop flow)

Fig. 28 shows the simulation results for one particular scenario in the random topology, with a varying data rate per flow. Simulation results for a highly loaded network are shown in the following section. As expected, simulation results are similar to those for the chain topology (see Figs. 26 and 27). That is, in Fig. 28 (a), the aggregate throughput for BASIC becomes relatively low, once the load becomes moderately high. PCM, PCM40, and 802.11 curves overlap in Fig. 28 (a).

Fig. 28 (b) shows the simulation results for the total data delivered per joule for the random topology with different data rates. When the data rate per flow is more than 20 Kbps, the BASIC scheme performs worse than 802.11 due to additional collisions and retransmissions. However, in Fig. 28 (b), PCM always performs better than 802.11 or BASIC. Similar to the simulation results for the chain topology, PCM40 results in a smaller amount of data delivered per joule compared to PCM, but it still performs better than 802.11 or BASIC in Fig. 28 (b).

d. Random Topology: 50 Different Topologies (one hop flow)

Fig. 29 shows the simulation results for a random topology with 50 flows. Each flow generates traffic at a rate of 1 Mbps; the network is overloaded. The numbers on the horizontal axis indicate 50 different scenarios (or topologies).

In Fig. 29 (a), PCM and PCM40 achieve throughput very close to 802.11 in every scenario, while BASIC performs poorly.

The poor aggregate throughput of the BASIC scheme results in poor data delivered per unit of energy consumption. Simulation results for the total data delivered per joule in Fig. 29 (b) show that PCM performs better than 802.11 or BASIC. As explained in Fig. 28 (b), PCM40 results in a smaller amount of data delivered per joule compared to

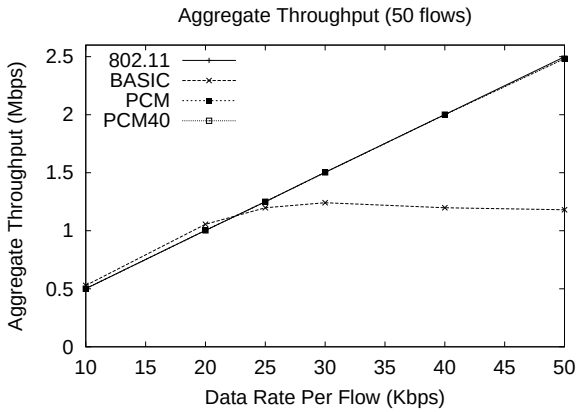

(a) Aggregate throughput

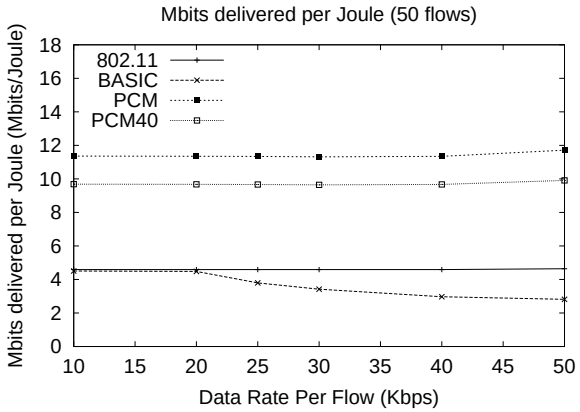

(b) Total data delivered per joule

Fig. 28. Random topology with different network loads: the curves for PCM, PCM40, and 802.11 overlap in (a).

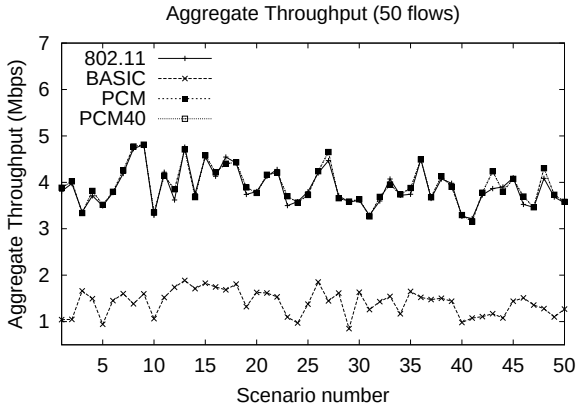

(a) Aggregate throughput

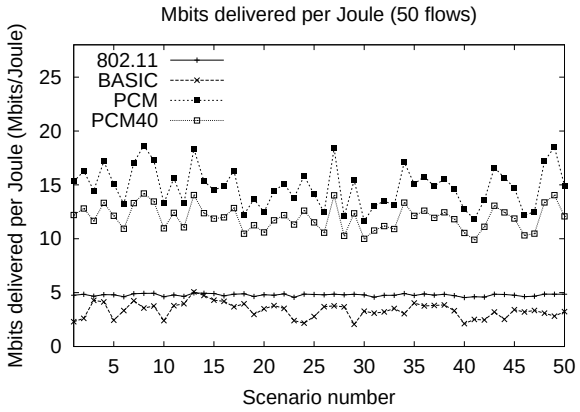

(b) Total data delivered per joule

Fig. 29. Random topology with one hop flows for 50 different scenarios using a 1 Mbps data rate per flow. The curves for PCM, PCM40, and 802.11 overlap in (a).

PCM, but it still performs better than 802.11 or BASIC in Fig. 29 (b).

e. Random Topology: Varying Packet Size (one hop flow)

Fig. 30 shows the simulation results for a random topology with 50 flows varying the packet size. Simulated packet sizes are 64, 128, 256, and 512 bytes. Each flow generates traffic at a rate of 50 Kbps.

The RTS/CTS overhead per packet is independent of the packet size. Therefore, as expected, when the packet size increases in Fig. 30 (a), the aggregate throughput of all schemes also increases. The curves for PCM and PCM40 overlap in Fig. 30 (a). PCM and PCM40 perform similar to 802.11 but BASIC performs poorly.

For the total data delivered per joule in Fig. 30 (b), PCM performs better than all other schemes. Also, the gap between PCM and BASIC (or 802.11) becomes bigger, as the packet size increases. This is because using a large packet size PCM has more time to use lower power during DATA transmission, thus conserving more energy. PCM40 also performs better than BASIC and 802.11 in terms of the total data delivered per joule.

f. Random Topology: 50 Different Topologies (multi-hop flow)

Fig. 31 shows the simulation results for a random topology with 30 multi-hop flows. Each flow generates traffic at a rate of 1 Mbps. The numbers on the horizontal axis indicate 50 different scenarios (or topologies). In Fig. 31 (a), PCM and PCM40 achieve throughput very close to 802.11 in every scenario, while BASIC performs poorly.

The poor aggregate throughput of the BASIC scheme results in poor data delivered per unit of energy consumption. Simulation results for the total data delivered per joule in Fig. 31 (b) show that PCM performs better than 802.11 or BASIC. As we saw in the earlier simulation results, PCM40 results in a smaller amount of data delivered per joule compared to PCM, but it still performs better than 802.11 or BASIC in Fig. 31 (b).

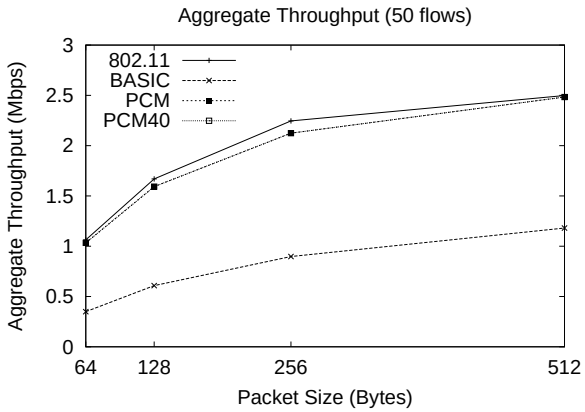

(a) Aggregate throughput

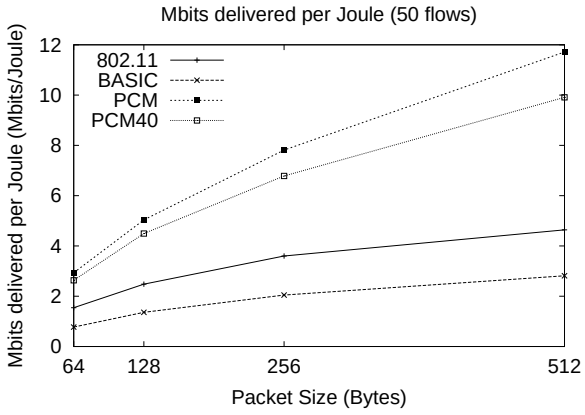

(b) Total data delivered per joule

Fig. 30. A random topology with different packet sizes and a 50 Kbps data rate per flow. PCM and PCM40 curves are overlapped in (a).

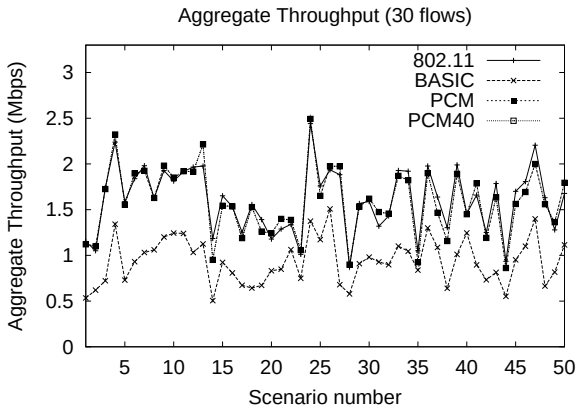

(a) Aggregate throughput

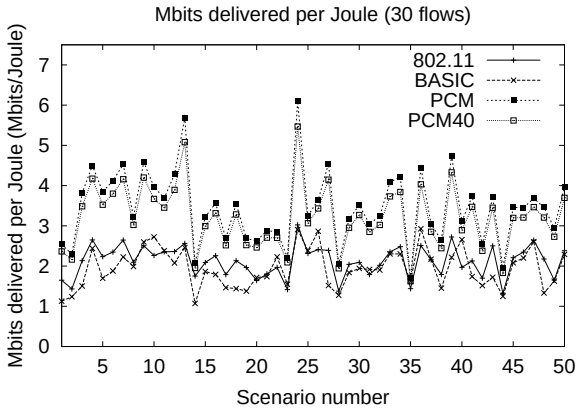

(b) Total data delivered per joule

Fig. 31. Random topology with multi-hop flows for 50 different scenarios using a 1 Mbps data rate per flow. The curves for PCM, PCM40, and 802.11 overlap in (a).

F. Summary

In the past, MAC protocols that use the maximum transmission power for RTS-CTS and the minimum necessary transmission power for DATA-ACK have been proposed with the goal of achieving energy saving. We refer to this as the BASIC scheme. However, we have shown that the BASIC scheme increases collisions and retransmissions, which can result in more energy consumption, and throughput degradation.

In IEEE 802.11, carrier sensing range for RTS-CTS is the same as that of DATA-ACK since transmission power does not change. However, in BASIC, carrier sensing range for RTS-CTS and DATA-ACK may vary because the transmission power can be different for those packets. Thus, when using BASIC, nodes in the carrier sensing zone of RTS-CTS can cause collisions with on-going DATA-ACK transmissions because these nodes may not sense DATA transmission which may use a lower transmission power. Such collisions trigger retransmissions, consuming more energy. Due to this, the BASIC scheme often yields an aggregate throughput and total data delivered per joule worse than IEEE 802.11 without power control.

We propose PCM, a Power Control MAC protocol, which periodically increases the transmission power during DATA transmission. Simulation results show that PCM achieves energy savings without causing throughput degradation.

One possible concern with PCM is that it requires a frequent increase and decrease in the transmission power which may make the implementation difficult. An alternative approach is to replace this higher power level for data by a busy tone at p_{max} in a separate channel, with one channel being used for the busy tone and the another channel for RTS-CTS-DATA-ACK. Another concern is that fading may adversely affect the PCM performance. As a variation of PCM, a different time interval can also be used between the transmissions at p_{max} during a packet transmission. In this variation, there is a trade-off

between performance and energy savings.

Although PCM provides energy saving it does not yield improved spatial reuse as compared to IEEE 802.11. Future work includes the development of a power control MAC protocol that conserves energy while increasing spatial reuse, preferably, without using a separate control channel.

CHAPTER IV

POWER AWARE ROUTING USING POWER CONTROL IN AD HOC NETWORKS

Since energy conservation is not an issue of one particular layer of the network protocol stack, many researchers have focused on cross layer designs to conserve energy more effectively. One such effort is to employ power control at the MAC layer and to design power aware routing at the network layer.

The BASIC power control protocol, discussed in Chapter III, has been used with power aware routing protocols to improve the energy efficiency. For example, power aware routing protocols in [12, 19] select a path that minimizes the aggregate transmission power consumed by all nodes on the path. It has been believed that those power aware routing protocols with BASIC-like power control can save energy as compared to the conventional routing, which uses the shortest number of hops as a routing metric. In this dissertation, however, we show contradicting results. That is, the power aware routing with BASIC-like power control degrades the network throughput as compared to IEEE 802.11 without power control. In addition, we also show the power aware routing protocol cannot achieve energy savings.

The rest of this chapter is organized as follows. Section A reviews the related work. Section B presents an overview of power aware routing with BASIC-like power control and investigates its energy efficiency. Section C describes our simulation model and discusses the simulation results. Section D summarizes this chapter.

A. Related Work

BASIC-like power control has been widely used for the purpose of energy conservation [19, 28, 40]. The deficiency of the BASIC protocol was addressed in Chapter III, where we

proposed a solution, called PCM (Power Control MAC).

Combined with the BASIC-like power control MAC protocols, power aware routing protocols have been studied to enhance energy savings. One such effort is PARO (Power Aware Routing Optimization) [19], which uses the BASIC protocol for its MAC protocol. For a routing metric, PARO chooses a path that minimizes the total transmission power consumed by all nodes on the path. Thus, when using PARO it is likely to have more hops than when using a conventional routing protocol with the shortest number of hops.

Doshi *et al.* [12] implemented an on-demand minimum energy routing protocol based on DSR [25]. Like PARO, this protocol also uses the metric that minimizes the total transmission power with BASIC-like power control.

A limitation of a power aware routing protocol with BASIC-like power control is discussed in [30]. The authors point out that the network throughput with BASIC can be degraded if packets traverse more hops. That is, when an intermediate node forwards packets, its neighbors have to defer their transmissions, which may cause throughput degradation. We will elaborate this limitation in Section 2. In this dissertation, we identify a more fundamental problem of the combination of a power aware routing and BASIC-like power control.

Several power aware routing metrics are presented in [47]. Among the metrics, the authors emphasize metrics that are represented as a function of remaining battery power in order to extend the network lifetime. They show a routing protocol using these metrics can reduce the cost per packet over the shortest hop routing.

CMMBER (Conditional Max-Min Battery Capacity Routing) [50] is a maximum battery life routing protocol, which tries to not only minimize the overall transmission power but also avoid the use of nodes that have low battery capacity. In CMMBER, if a route from a source to a destination contains nodes with low battery capacity (below a threshold), the route is avoided to extend the network lifetime. On the other hand, if every node in some

possible routes has sufficient remaining battery capacity, then a path that minimizes the total transmission power is chosen.

Another protocol to extend the network lifetime is proposed in [42]. Using the location information, the protocol chooses a path that minimizes the energy consumed to deliver a packet. A zone-based online power-aware routing protocol is proposed in [34], which also seeks to optimize the network lifetime.

Other optimizations also include topology control [41, 42, 43, 52], energy efficient spanning trees for multicasting and broadcasting [53, 54], and using power saving mode at the MAC layer [7, 58, 60].

B. Power Aware Routing Using Power Control

1. An Overview of Power Aware Routing Optimization

In this section we briefly overview how PARO [19] works. We study PARO as an example of power aware routing with BASIC-like power control, which selects the minimum total transmission power path. PARO has 3 core algorithms: overhearing algorithm, redirection algorithm, and route-maintenance algorithm for mobility.

The overhearing algorithm handles packets that are received by the MAC successfully. When a node overhears a packet from its neighbor, it creates an entry in the “overhear table” or refreshes the entry if the entry for the neighbor already exists. The entry includes the minimum transmission power necessary to communicate with the neighbor based on the signal strength of the received packet and the power level at which the packet was sent. The information of the latter is included inside the packet by the sender.

The redirection algorithm performs the route optimization, which leads to discovering paths that require less transmission power to forward a packet. Using the overhearing algorithm, if a node finds a path that consumes less transmission energy, the node becomes

a redirector and transmits a redirect message to the sender. The redirect message includes a new energy efficient path.

Since only one intermediate node (redirector) can be added in a path at a time, PARO optimizes routes one step at a time. Therefore, the number of iterations required to reach an optimum route is the same as the number of redirectors included in the route.

The route maintenance algorithm is designed for a network where nodes are mobile. PARO relies on data packets to maintain route information. In case of node mobility, route information may become stale if there is no data traffic. In PARO, source nodes transmit *route-maintenance* packets to destination nodes whenever there is no data packet to send for a fixed time interval named *route-timeout*. When nodes receive or overhear these packets, they update routing information to maintain fresh routes.

2. Energy Efficiency of PARO

We first show the performance of PARO with a simple scenario depicted in Fig. 32. It is a simple chain topology which consists of 3 nodes. Nodes are shown as a circle, and the arrow between two nodes indicates a traffic flow. For this specific topology, node A is a source that transmits packets to node C. The distance between adjacent node pairs is 50 m.

In Fig. 32, node A can either send a packet directly to node C by using the shortest path routing or forward them through an intermediate node B by using PARO. The dashed line from A to C in Fig. 32 indicates the former case while the two other flows (A-B and C-D) indicate the latter.

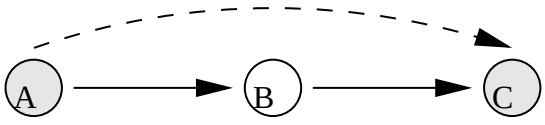

Fig. 32. Chain topology: node A can transmit packets to node C directly, or forward them through an intermediate node B.

Fig. 33 shows simulation results of the chain topology. We will use the following to describe the protocols used in graphs in this chapter:

- *R-802.11*: IEEE 802.11 MAC without power control using the shortest path routing.
- *PARO*: power aware routing with BASIC-like power control. For a simulation purpose, PCM (Power Control MAC) from Chapter III is used as the BASIC-like power control protocol.
- *R-PCM*: PCM with shortest path routing.
- *R-PCMO*: PCM with an Option; this will be elaborated below in Section 3.

Note that R-802.11, R-PCM, and R-PCMO use the shortest path routing while PARO uses the power aware routing.

Fig. 33 (a) shows the aggregate throughput of R-802.11, PARO, and R-PCM on the chain topology depicted in Fig. 32. The horizontal axis represents data rate per flow in Kbps, and the vertical axis represents the corresponding aggregate throughput achieved by R-802.11, PARO, and R-PCM. The graphs for R-802.11 and R-PCM are overlapped. When the network load is low, the aggregate throughput of all schemes perform the same. However, the aggregate throughput of PARO starts suffering at 700 Kbps per flow and does not increase beyond 600 Kbps. Since BASIC-like power control uses the maximum transmission power for RTS and CTS, all nodes (A, B, and C) in Fig. 32 are within their transmission ranges. When PARO is used, A will transmit packets to B and then B will forward them to C. In this situation, two flows (A-B and B-C) share bandwidth and they contend with each other for channel bandwidth; this results in low throughput. As studied in [33], this is not a surprising result. As the expected path length increases, the bandwidth available for each node to originate packets decreases. However, this is overlooked in [12, 19], focusing only on the aspect of energy consumption.

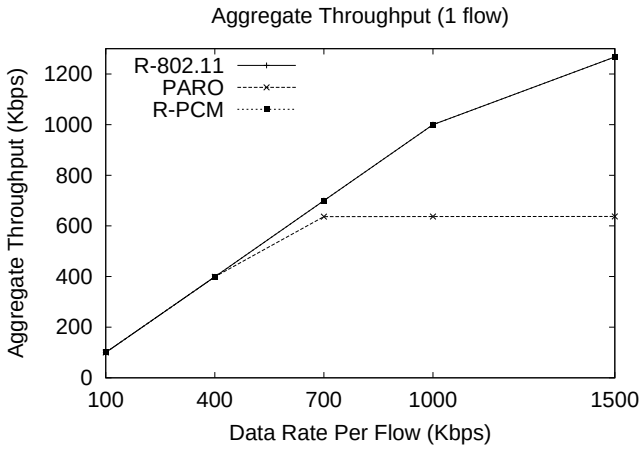

(a) Aggregate throughput

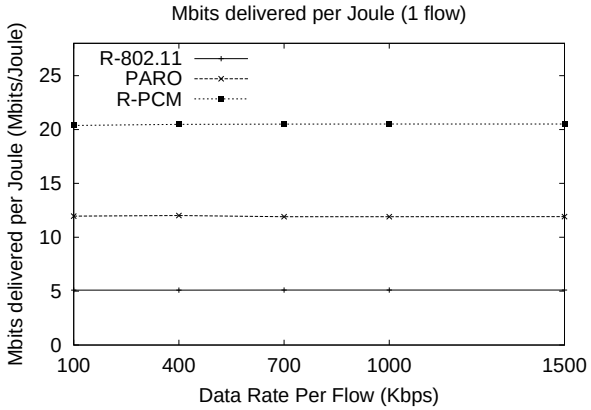

(b) Total data delivered per joule

Fig. 33. Chain topology: the curves for R-PCM and R-802.11 overlap in (a). The aggregate throughput of PARO does not increase beyond 600Kpbs due to the contention between two flows.

Fig. 33 (b) shows the total data delivered per unit of transmission energy by R-802.11, PARO, and R-PCM. The horizontal axis represents data rate per flow in Kbps and the vertical axis represents the corresponding data delivered per unit of transmission energy. Since R-PCM uses the minimum necessary transmission power for data transmissions between A and C (which are 100 m apart), it achieves more energy savings than R-802.11. PARO also performs better than R-802.11. However, it is important to note that R-PCM performs better than PARO. In PARO, packets traverse more hops – a process in which RTS and CTS are sent at the maximum transmission power in each hop. Also, there is extra energy consumption associated with transmitting more RTS and CTS. Furthermore, since there is no spatial reuse in PARO, more flows from a source to a destination will contend each other. This can cause packet retransmissions which leads to more energy consumption. More specifically, in our simulations, PARO uses the maximum transmission power (0.2818 W) for RTS-CTS and the minimum necessary transmission power (0.002 W) for DATA-ACK. The power consumption is multiplied by 2 since the packet is forwarded by node B. Similarly, R-PCM uses the maximum transmission power (0.2818 W) for RTS-CTS and the minimum necessary transmission power (0.015 W) for DATA-ACK. Also, both PARO and R-PCM consume the maximum transmission power for periodic power increment during data packet transmission.

From the simple chain topology, we show that the power aware routing with BASIC-like power control may not be as energy efficient as R-PCM with the shortest path routing. This is mainly because there is no spatial reuse in BASIC-like power control – if a packet traverses more hops it results in lower throughput.

Another potential problem of a power aware routing with BASIC-like power control is discussed in [30]. Let us consider the scenario in Fig. 34. Nodes A, B, and C are within the transmission ranges of each other. Node D is within B's transmission range but outside the transmission ranges of A and C. When PARO is used, packets from A to C will be

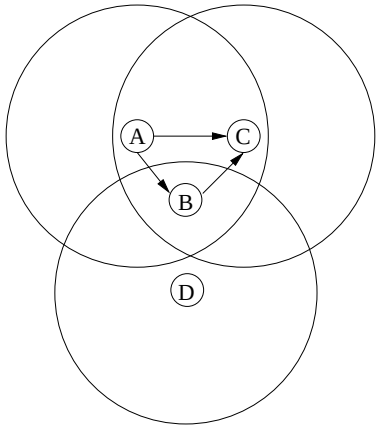

Fig. 34. A limitation of a power aware routing protocol with BASIC-like power control: when B is forwarding packets for nodes A and C, D has to defer its transmission, which can cause throughput degradation.

transmitted via B. Thus, when B is forwarding packets for A and C, node D has to defer its transmission. This may cause lower network throughput than that with the conventional routing protocol. This problem will not appear if there is no traffic through D. As we described in this dissertation, a more fundamental problem here is the contention between two flows, A–B and B–C.

3. Overhearing Process with Power Control

In PARO, the overhearing algorithm is used to find paths that require less transmission power consumption to forward a packet. By overhearing neighbors' transmissions, a route can be optimized.

In general, the overhearing algorithm can also be used in a conventional routing protocol to find the shortest path. For instance, in DSR [25] the overhearing algorithm is performed in promiscuous listening mode; that is, when a node overhears a packet, it can learn paths between nodes even though it may not be a part of the path. Once overhearing a packet, the node looks up its route cache to see if it has a shorter path. If so, it sends a

RREP (Route Reply) packet to the sender to notify a new route.

However, the overhearing algorithm may not be performed as expected if it is used with power control. That is, when power control is used, a packet is sent at the minimum necessary transmission power. Thus, the number of neighbors that can overhear the packet is reduced. When compared with R-802.11, R-PCM (and also PARO) uses longer paths since the overhearing algorithm is not used as much. As discussed with PARO, using longer paths can degrade the aggregate throughput, which results in poor energy efficiency. This side effect appeared during our simulations. We fix this problem by having all nodes in the network periodically not use power control – that is, all nodes periodically use the maximum transmission power. With this simple modification, the overhearing process can be performed by all nodes in the network periodically. We include this modification in our simulations as an option for R-PCM, which is indicated as R-PCMO (PCM with Option). Specifically, in our simulation, nodes give up power control every one second for a duration of 50 $msec$. Note that since this option forces all nodes to uses the maximum transmission power periodically, the power consumption using this option will be slightly higher than that of R-PCM.

Along with the above modification, we also make the nodes use the maximum transmission power for all the routing control packets, such as RREQ (Route Request), RREP (Route Reply), and RRER (Route Error). Therefore, routing information will be overheard by all the neighbors, and route discovery or maintenance will not be affected by power control. In the following section, we show more simulation results for various scenarios.

C. Performance Evaluation

We simulate PARO [19], which selects the minimum energy path using BASIC-like power control, PCM (Power Control MAC) using the shortest path routing, PCM with the Option

using the shortest path routing, and IEEE 802.11 with the shortest path routing without power control. In the graphs we indicate these protocols as PARO, R-PCM, R-PCMO, and R-802.11, respectively. We use the following metrics to evaluate these schemes:

- *Aggregate throughput over all flows in the network.*
- *Total data delivered per unit of transmission energy consumption (Mbits delivered per joule).*

1. Simulation Model

We use ns-2 with the CMU wireless extensions [10] for our simulations. The duration of each simulation is 20 seconds. We perform simulations using both CBR (Constant Bit Rate) and TCP traffic. Each flow transmits either CBR or TCP. For CBR, the rate of traffic is varied in different simulations. TCP flow is generated by FTP applications. The channel bit rate is 2 Mbps, and the packet size is fixed at 512 bytes. Each node starts with enough energy so that it will not run out of its energy during the simulations. All simulation results are the average of 30 runs.

As in Chapter III, we consider four transmission power levels, 2 mW, 15 mW, 75.8 mW, and 281.8 mW, roughly corresponding to the transmission ranges of 60 m, 120 m, 180 m, and 250 m, respectively.

For the random topologies, we first simulate with 30 nodes in a 100 x 100 m^2 area, which is the same size as that used in PARO. For each scenario, 10 source and 10 destination nodes are randomly chosen. In addition, we simulate another random topology with a larger network, where 50 nodes are randomly placed in a 1000 x 1000 m^2 area. Like the scenario with 30 nodes, 10 source and 10 destination nodes are randomly chosen among 50 nodes. Also, we simulate a congested network with more flows, where 20 source and 20 destination nodes are randomly chosen among 50 nodes. Note that in all scenarios, any

source or destination node can also be an intermediate node that forwards traffic for other nodes.

2. Simulation Results

a. Random Topology: 30 Nodes in 100 x 100 m^2

Fig. 35 shows the simulation results of a random topology with 30 nodes in a 100 x 100 m^2 area. Ten source and ten destination nodes are randomly chosen. Each flow transmits CBR traffic, and the rate of each traffic flow is varied from 2 Kbps to 50 Kbps as plotted on the horizontal axis in Fig. 35. The corresponding aggregate throughput and the data delivered per unit of transmission energy are shown on the vertical axis of the graphs in Fig. 35 (a) and (b), respectively.

In Fig. 35 (a), the aggregate throughput of all schemes are the same – all curves are overlapped. PARO performs better than R-802.11 in terms of energy efficiency in Fig. 35 (b) as in [19]. However, as we explained in the chain topology in Fig. 33, PARO performs worse than R-PCM due to the channel contention among flows. As mentioned earlier, if using BASIC-like power control, there are less nodes that can overhear a packet since data packets are sent at the minimum necessary transmission power. Thus, a selected route in PARO may be longer than the shortest path. R-PCMO, which uses the maximum transmission power periodically, performs slightly better than R-PCM in Fig. 35 (b). In R-PCMO more nodes may overhear packet transmissions so a route can be optimized to be the shortest path. As we shall see in next section, PARO does not save energy all the time – it can even consume more energy than R-802.11 without power control.

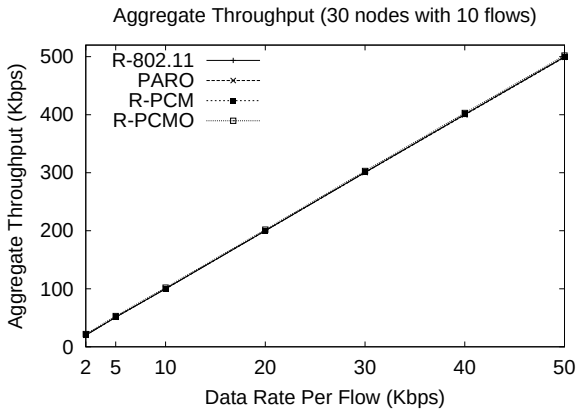

(a) Aggregate throughput

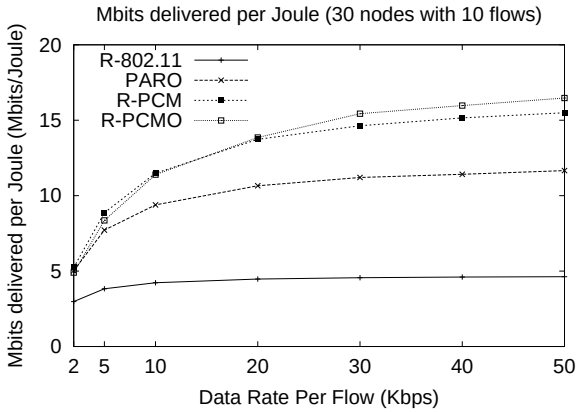

(b) Total data delivered per joule

Fig. 35. Random topology with different network loads (30 nodes in 100 x 100m^2): the curves for R-PCM, PARO, and R-802.11 overlap in (a).

b. Random Topology: 50 Nodes in 1000 x 1000 m^2

We now present simulation results of a random topology with 50 nodes in a 1000 x 1000 m^2 area, varying network load and the number of traffic flows.

Fig. 36 shows the simulation results, where 10 source and 10 destination nodes are randomly chosen among 50 nodes. Fig. 37 shows simulation results for 20 flows – 20 sources and 20 destinations are randomly selected.

In Figs. 36 (a) and 37 (a), as the network load gets higher, the aggregate throughput of PARO gets lower than that of R-PCM or R-802.11. This is similar to Fig. 33 (a). BASIC-like power control offers no spatial reuse. Besides, in PARO, packets tend to traverse longer hops, which leads to more contentions among flows from a source to a destination. Therefore, the throughput achieved by PARO is lower than other schemes, especially at high load.

One more observation is that the aggregate throughput of R-PCM in Fig. 36 (a) is slightly lower than that of R-802.11 at 50 Kbps data rate per flow. Similarly, in Fig. 37 (a) the aggregate throughput of R-PCM is lower than R-802.11 at 25 or 30 Kbps. As explained earlier, the overhearing algorithm may be performed by fewer nodes in BASIC-like power control since data packets are transmitted at the minimum necessary transmission power. Thus, paths used in BASIC-like power control can be longer than the shortest path, which can result in a low throughput at high load. R-PCMO achieves the same aggregate throughput in Figs. 36 (a) and 37 (a) by having all nodes use the maximum transmission power periodically.

Figs. 36 (b) and 37 (b) show the total data delivered per unit of transmission energy in the random topology using 10 flows and 20 flows, respectively. The energy savings achieved by PARO is lower than that of R-802.11. R-PCM conserves more energy as compared to PARO or R-802.11. At high load, R-PCMO performs slightly better than

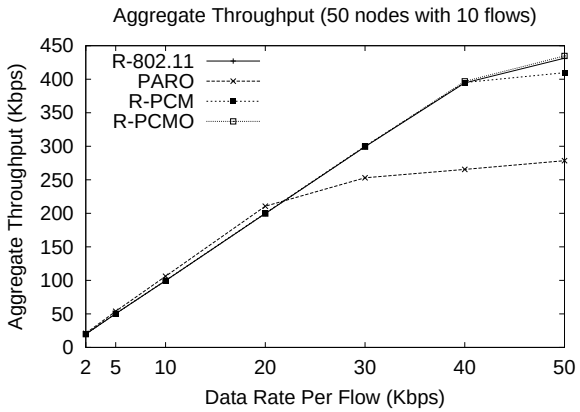

(a) Aggregate throughput

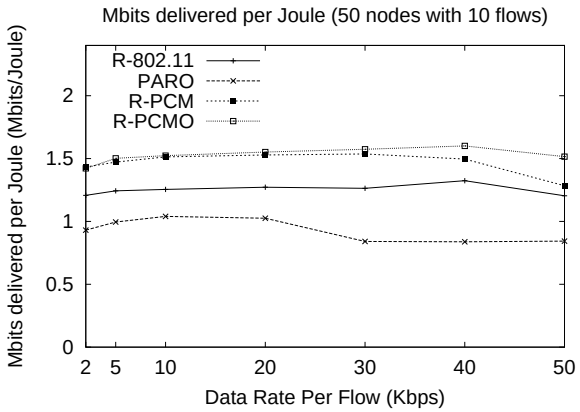

(b) Total data delivered per joule

Fig. 36. Random topology with different network loads (50 nodes with 10 flows in 1000 x 1000m^2).

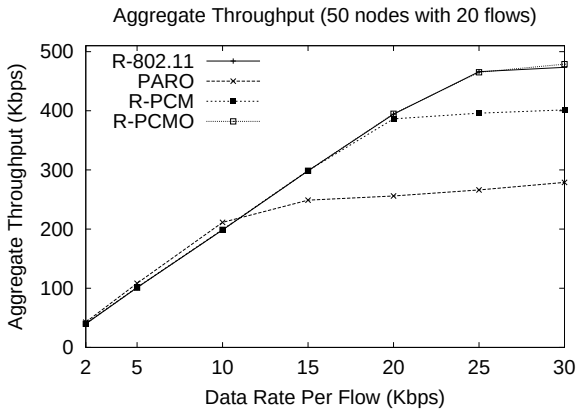

(a) Aggregate throughput

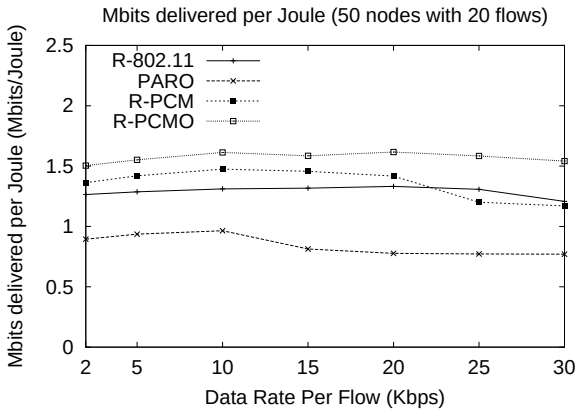

(b) Total data delivered per joule

Fig. 37. Random topology with different network loads (50 nodes with 20 flows in 1000 x 1000m^2).

R-PCM.

c. More Simulation Results in 1000 x 1000 m^2

We now present more simulation results for a random topology with 50 different scenarios in a 1000 x 1000m^2 area. Fig. 38 shows the simulation results for 50 nodes with 10 flows. The data rate of each traffic flow is fixed at 50 Kbps. The numbers on the horizontal axis indicate 50 different scenarios (or topologies). The simulation result for each scenario is the average of 30 runs. Fig. 39 is the same graph, but each value in all schemes is normalized (divided) by the value achieved by R-PCMO.

For example, in Fig. 39 (a), a value for PARO indicates an aggregate throughput achieved by PARO divided by that of R-PCMO. Therefore, if a value in Fig. 39 is greater than 1, it means that the corresponding scheme performs better than R-PCMO. On the other hand, if it is less than 1, it means that the corresponding scheme performs worse than R-PCMO. If a value is around 1, it means that the scheme performs similar to R-PCMO.

As we saw in other graphs earlier (Figs. 33–37), in Figs. 38 (a) and 39 (a), PARO achieves poor aggregate throughput as compared to R-PCM and R-802.11. The performance of R-PCM, R-PCMO, and R-802.11 is similar.

In Figs. 38 (b) and 39 (b) the total data delivered per unit of transmission energy for PARO is lower than those of other schemes. R-PCM and R-PCMO perform similar to each other, which is better than PARO and R-802.11. Recall that R-PCMO makes all nodes in the network use the maximum transmission power periodically. Thus, if R-PCM and R-PCMO maintain the same route for all the network flows, R-PCMO will consume more energy than R-PCM.

Fig. 40 shows the simulation results when there are 20 flows in the network, and Fig. 41 is its normalized graph – each value is divided by the value achieved by R-PCMO. Fifty different scenarios are considered at the data rate of 25 Kbps. These graphs show

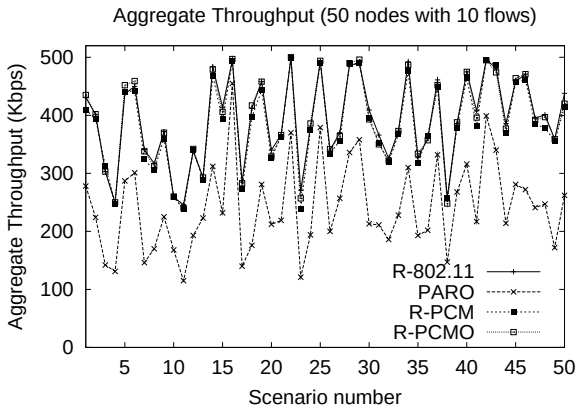

(a) Aggregate throughput

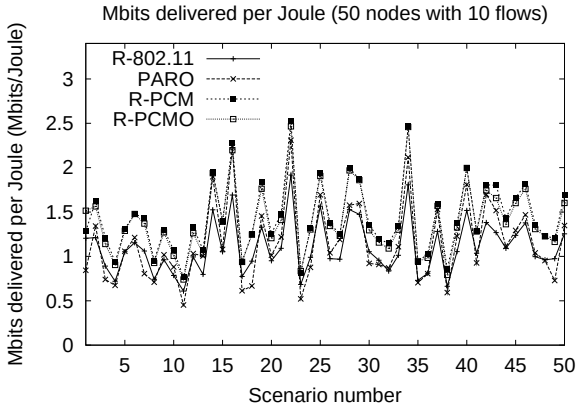

(b) Total data delivered per joule

Fig. 38. Random topology for 50 different scenarios with a 50 Kbps data rate per flow (50 nodes in 1000 x 1000m^2): 10 flows.

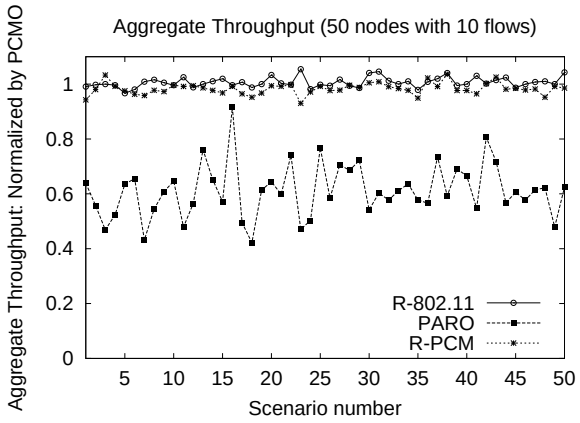

(a) Aggregate throughput: normalized

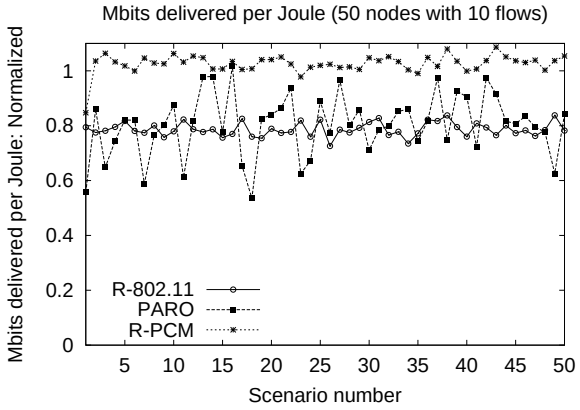

(b) Total data delivered per joule: normalized

Fig. 39. Random topology for 50 different scenarios with a 50 Kbps data rate per flow (50 nodes in 1000 x 1000m^2): 10 flows – normalized.

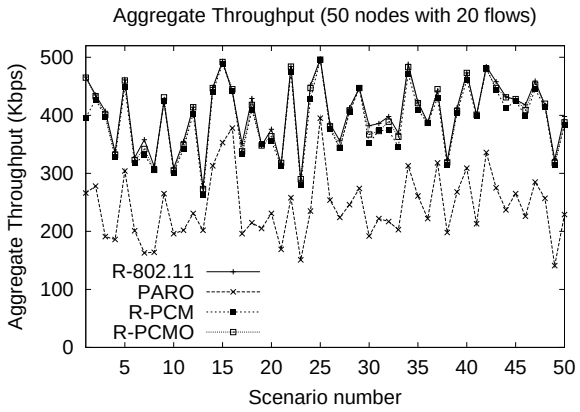

(a) Aggregate throughput

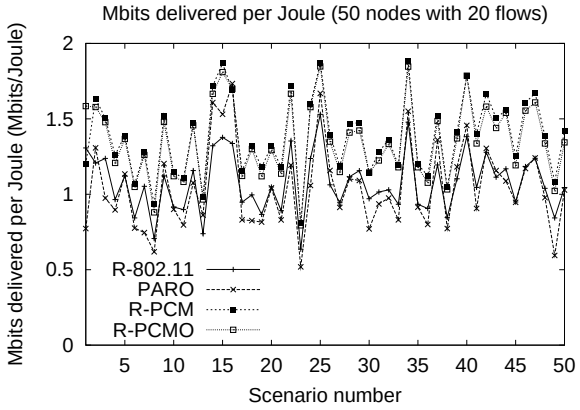

(b) Total data delivered per joule

Fig. 40. Random topology for 50 different scenarios with a 25 Kbps data rate per flow (50 nodes in 1000 x 1000m^2): 20 flows.

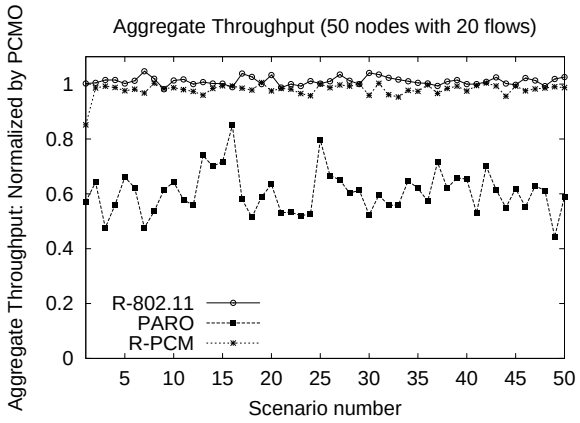

(a) Aggregate throughput: normalized

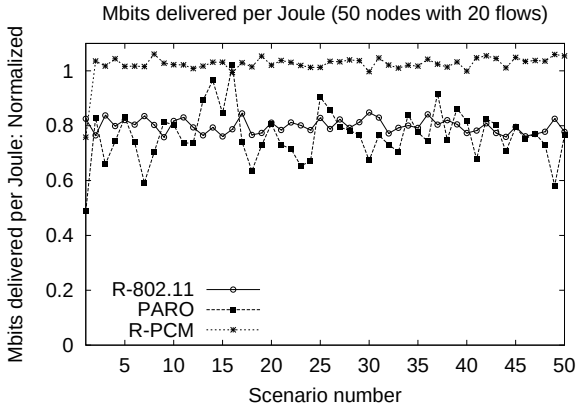

(b) Total data delivered per joule: normalized

Fig. 41. Random topology for 50 different scenarios with a 25 Kbps data rate per flow (50 nodes in 1000 x 1000m^2): 20 flows – normalized.

the same trends as Figs. 38 and 39. In Figs. 40 (a) and 41 (a), PARO has poor aggregate throughput as compared to R-PCM and R-802.11, and all other schemes perform the same. In Figs. 40 (b) and 41 (b), R-PCM and R-PCMO perform similar to each other, but their performances are better than PARO and R-802.11. PARO performs even worse than R-802.11.

d. TCP Simulation Results in 1000 x 1000 m^2

In this section, we present simulation results for TCP traffic. Like in the previous section, we simulate a random topology using 50 nodes with 10 flows. Fig. 42 shows the simulation results of 50 different scenarios in a 1000 x 1000m^2 area. Fig. 43 shows the same graph, but each value in all schemes is normalized (divided) by the value achieved by R-PCMO. As mentioned earlier, if a value in Fig. 43 is greater than 1, it means that the corresponding scheme performs better than R-PCMO. On the other hand, if it is less than 1, it means that the corresponding scheme performs worse than R-PCMO.

In Figs. 42 (a) and 43 (a), the aggregate throughput of PARO is worse than that of all other schemes. Although R-PCM performs better than PARO, its aggregate throughput is lower than that of R-PCMO or R-802.11. As explained before, in R-PCM nodes use the minimum necessary transmission power for data packets, therefore, the number of neighbors that can overhear routing packets is reduced. Because of this, nodes in R-PCM tends to use longer paths than R-802.11 degrading the network throughput. The aggregate throughput of R-PCMO is similar to that of R-802.11 most of the time, but sometimes it is slightly worse than R-802.11. Since R-PCMO uses the maximum transmission power periodically, there is more chances for nodes to overhear routing packets than R-PCM. However, there exists delay to overhear and update the routing information. During the time, nodes will use a longer path which can affect TCP throughput.

Figs. 42 (b) and 43 (b) show the total data delivered per unit of transmission of energy

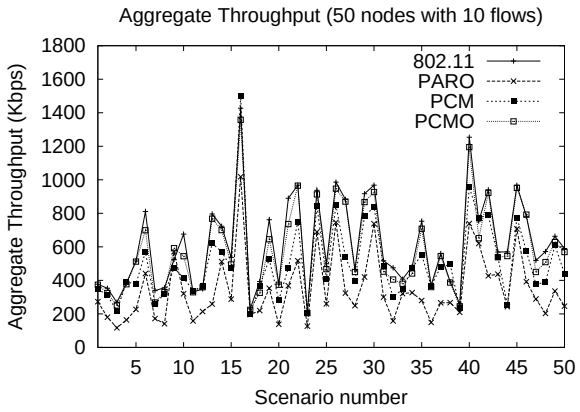

(a) Aggregate throughput

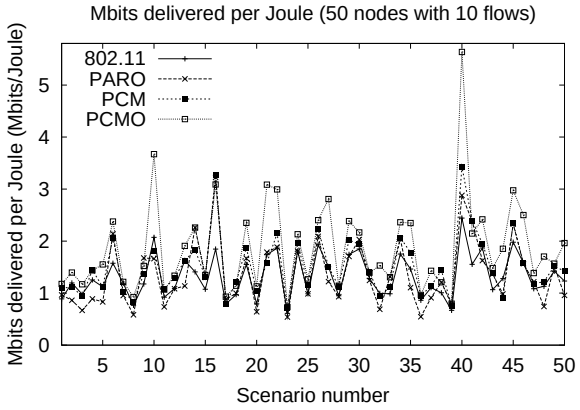

(b) Total data delivered per joule

Fig. 42. Random topology for 50 different scenarios with TCP traffic (50 nodes in 1000 x 1000m^2): 10 flows.

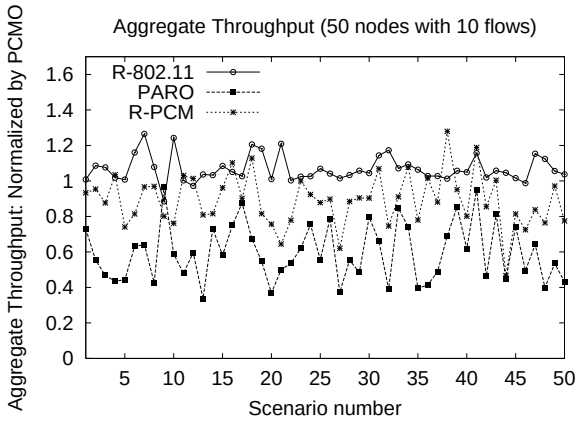

(a) Aggregate throughput: normalized

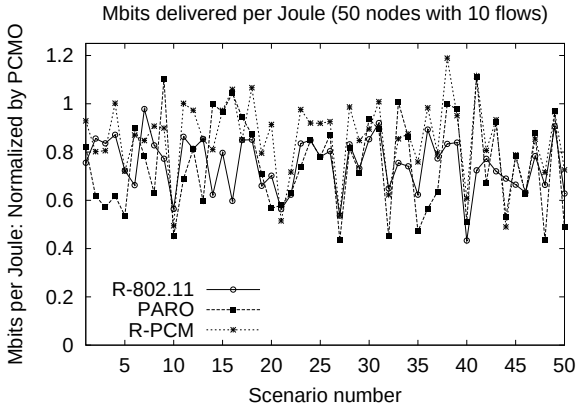

(b) Total data delivered per joule: normalized

Fig. 43. Random topology for 50 different scenarios with TCP traffic (50 nodes in 1000 x 1000m^2): 10 flows – normalized.

for TCP traffic. R-PCMO performs slightly better than all other schemes. Due to the low throughput, PARO performs the worst. However, the differences among all schemes are not significant.

D. Summary

A power aware routing, which minimizes the total transmission power, with BASIC-like power control has been considered energy efficient. In this chapter we use PARO as an example. Contrary to previous studies such as PARO, we have shown that the power aware routing with BASIC-like power control is not energy efficient – it may even consume more energy as compared to IEEE 802.11 without power control. As compared to the shortest path routing, the power aware routing forces a packet to traverse more hops, with the minimum necessary transmission power in each hop, from a source to a destination. Since BASIC-like power control does not provide spatial reuse, as a packet traverses longer hops, it creates an overhead. That is, all flows on a single path have to share the channel bandwidth and contend with each other to forward a single packet. Therefore, the aggregate throughput achieved by PARO is much lower than that of IEEE 802.11 without power control. This becomes a serious problem especially when the network load is high. Due to the poor throughput, the energy savings achieved by PARO is low. This is simple and obvious but has been entirely overlooked in the past.

We have shown that the shortest path routing with BASIC-like power control performs more energy efficiently than both PARO and IEEE 802.11. We have also found that using BASIC-like power control, it is possible for the aggregate throughput to degrade. Since data packets are sent at the minimum necessary transmission power, there can be less nodes that overhear data packets. This can result in using a longer path than the shortest path. This problem can be fixed by forcing every node in the network to use the maximum

transmission power periodically so that all nodes can overhear more packet transmissions to find the shortest path.

CHAPTER V

CONCLUSION

Energy efficiency is an important issue in the design of wireless networks. In this dissertation we have studied two approaches to conserve energy and their interactions with other layers. In this chapter, we summarize our contributions and conclude the dissertation by discussing future research.

A. Contributions

- We identified that the PSM specified for DCF in an IBSS of IEEE 802.11 does not always perform well because of its fixed ATIM window size. We proposed an adaptive scheme that allows a node to dynamically adapt its ATIM window size based on observed network conditions. The proposed scheme also allows a node to power off its wireless network interface whenever it finishes packet transmission for the announced packets. These two lead to a throughput comparable to that of IEEE 802.11 without power saving mode and significant energy savings as comparable to the PSM of IEEE 802.11, respectively. We also found that power saving mode does not perform well with TCP traffic. We showed that nodes can achieve energy savings without degrading throughput by temporarily giving up power saving mode when there exists TCP traffic in the network.
- We identified that the BASIC power control protocol has a deficiency that causes an increase in collisions and degrades network throughput. We proposed a power control scheme that fixes the above problem. Our simulation results show that the proposed scheme achieves energy savings without degrading throughput.
- We investigated the interaction between the power control MAC protocol and a power

aware routing protocol in ad hoc networks. Contrary to previous studies such as PARO, we showed that power aware routing with BASIC-like power control is not energy efficient. We showed that the shortest path routing with BASIC-like power control performs more energy efficiently than both PARO and IEEE 802.11.

B. Future Research

We studied power saving mode and power control in the context of IEEE 802.11, which is the most widely used wireless local area network (WLAN) technology. Energy efficiency is also a critical issue in other applications, such as sensor networks and ubiquitous computing. Devices used for these applications are different from those for MANET (Mobile Ad Hoc Networks) since they have more strict resource constraints – that is, they usually have limited memory capacity, computational capability, and battery power. Although many MAC protocols are proposed for MANET, the design of an efficient MAC protocol for other applications (like sensor networks) is still an open research issue.

The power control protocol proposed in this dissertation provides energy savings; however, it does not yield improved spatial reuse as compared to IEEE 802.11 without power control. Future work on this topic includes the development of a power control MAC protocol that conserves energy while increasing spatial reuse, preferably, without using a separate control channel.

About power aware routing, it is desirable to design a power aware routing protocol that provides more energy savings. It will also be interesting to see how the power aware routing performs with other types of power control that provide spatial reuse.

REFERENCES

[1] S. Agarwal, S. Krishnamurthy, R. H. Katz, and S. K. Dao, "Distributed Power Control in Ad-hoc Wireless Networks," in *Proceedings of the 15th IEEE International Symposium on Personal, Indoor and Mobile Radio Communications (PIMRC)*, San Diego, CA, vol. 2, September 2001, pp. 59–66.

[2] S. Agrawal and S. Singh, "An Experimental Study of TCP's Energy Consumption over a Wireless Link," in *Proceedings of the 4th European Personal Mobile Communications Conference*, Vienna, Austria, February 2001.

[3] C. Bisdikian, "An Overview of the Bluetooth Wireless Technology," *IEEE Communications Magazine*, vol. 39, December 2001, pp. 86–94.

[4] B. Burns and J.-P. Ebert, "Power Consumption, Throughput and Packet Error Measurements of an IEEE 802.11 WLAN Interface," Telecommunication Networks Group, Technische Universitt Berlin, Tech. Rep., August 2001.

[5] J. C. Cano and P. Manzoni, "Evaluating the Energy-Consumption Reduction in a MANET by Dynamically Switching-off Network Interfaces," in *Proceedings of the 6th IEEE Symposium on Computers and Communications*, Hammamet, Tunisia, July 2001, pp. 186–191.

[6] J.-H. Chang and L. Tassiulas, "Energy Conserving Routing in Wireless Ad-hoc Network," in *Proceedings of the IEEE International Conference on Computer Communications (INFOCOM)*, Tel Aviv, Israel, March 2000, pp. 22–31.

[7] B. Chen, K. Jamieson, H. Balakrishnan, and R. Morris, "Span: An Energy-Efficient Coordination Algorithm for Topology Maintenance in Ad Hoc Wireless Networks," in *Proceedings of the ACM International Conference on Mobile Computing and Networking (MOBICOM)*, Rome, Italy, July 2001, pp. 85–96.

[8] A. Chockalingam and M. Zorzi, “Energy Efficiency of Media Access Protocols for Mobile Data Networks,” *IEEE Transactions on Communications*, vol. 46, November 1998, pp. 1418–1421.

[9] J.-M. Choi, Y.-B. Ko, and J.-H. Kim, “Enhanced Power Saving Scheme for IEEE 802.11 DCF Based Wireless Networks,” in *Proceedings of the IFIP International Conference on Personal Wireless Communication*, Athens, Greece, September 2003, pp. 835–840.

[10] CMU Monarch Project, “Extension to the NS Simulator.” Accessed: March 2005, http://www.monarch.cs.cmu.edu/cmu-ns.html.

[11] J. Deng and Z. J. Haas, “Dual Busy Tone Multiple Access (DBTMA): A New Medium Access Control for Packet Radio Networks,” in *IEEE International Conference on Universal Personal Communications (ICUPC ’98)*, Florence, Italy, vol. 2, May 1998, pp. 973–977.

[12] S. Doshi, S. Bhandare, and T. X. Brown, “An On-demand Minimum Energy Routing Protocol for a Wireless Ad Hoc Network,” *Mobile Computing and Communications Review*, vol. 6, July 2002, pp. 50–66.

[13] J.-P. Ebert, B. Stremmel, E. Wiederhold, and A. Wolisz, “An Energy-efficient Power Control Approach for WLANs,” *Journal of Communications and Networks (JCN)*, vol. 2, September 2000, pp. 197–206.

[14] J.-P. Ebert and A. Wolisz, “Combined Tuning of RF Power and Medium Access Control for WLANs,” in *Proceedings of the IEEE International Workshop on Mobile Multimedia Communications (MoMuC)*, San Diego, CA, November 1999, pp. 74–82.

[15] L. M. Feeney, “An Energy-consumtion Model for Performance Analysis of Routing Protocols for Mobile Ad Hoc Networks,” *Baltzer/ACM Journal of Mobile Networks*

and Applications (MONET) Special Issue on "QoS in Heterogeneous Wireless Networks", vol. 6, June 2001, pp. 239–249.

[16] L. M. Feeney and M. Nilsson, "Investigating the Energy Consumption of a Wireless Network Interface in an Ad Hoc Networking Environment," in *Proceedings of the IEEE International Conference on Computer Communications (INFOCOM)*, Anchorage, AK, April 2001, pp. 1548–1557.

[17] J. Gomez, A. T. Campbell, M. Naghshineh, and C. Bisdikian, "PARO: Power-aware Routing in Wireless Packet Networks," in *Proceedings of the IEEE International Workshop on Mobile Multimedia Communications (MoMuC)*, San Diego, CA, November 1999, pp. 380–383.

[18] J. Gomez, A. T. Campbell, M. Naghshineh, and C. Bisdikian, "Conserving Transmission Power in Wireless Ad Hoc Networks," in *Proceedings of the IEEE International Conference on Network Protocols (ICNP)*, Riverside, CA, November 2001, pp. 24–34.

[19] J. Gomez, A. T. Campbell, M. Naghshineh, and C. Bisdikian, "PARO: Supporting Dynamic Power Controlled Routing in Wireless Ad Hoc Networks," *ACM/Kluwer Journal on Wireless Networks (WINET)*, vol. 9, September 2003, pp. 443–460.

[20] Z. J. Haas and J. Deng, "Dual Busy Tone Multiple Access (DBTMA)–Performance Evaluation," in *Proceedings of the Annual Vehicular Technology Conference*, Houston, TX, vol. 1, 1999, pp. 314–319.

[21] P. J. M. Havinga and G. J. M. Smit, "Energy-efficient TDMA Medium Access Control Protocol Scheduling," in *Proceedings of Asian International Mobile Computing Conference (AMOC 2000)*, Penang, Malaysia, November 2000, pp. 1–9.

[22] W. R. Heinzelman, A. Chandrakasan, and H. Balakrishnan, "Energy-Efficient Com-

munication Protocol for Wireless Microsensor Networks," in *Proceedings of the 33rd IEEE Hawaii International Conference on System Sciences*, Maui, Hawaii, January 2000.

[23] IEEE, *Wireless LAN Medium Access Control (MAC) and Physical Layer (PHY) Specification*. New York: IEEE Press, November 1997.

[24] P. Johansson, R. Kapoor, M. Kazantzidis, and M. Gerla, "Rendezvous Scheduling in Bluetooth Scatternets," in *Proceedings of the IEEE International Conference on Communications (ICC)*, New York, vol. 1, April 2002, pp. 318–324.

[25] D. B. Johnson and D. A. Maltz, "Dynamic source routing in ad hoc wireless networks," in *Mobile Computing*, T. Imielinski and H. Korth, eds., Norwell, MA: Kluwer Academic Publishers, 1996, pp. 153–181.

[26] E.-S. Jung and N. H. Vaidya, "A Power Control MAC Protocol for Ad Hoc Networks," *ACM/Kluwer Journal on Wireless Networks (WINET)*, vol. 11, January 2005, pp. 55–66.

[27] A. Kamerman and L. Monteban, "WaveLAN-II: A High-Performance Wireless LAN for the Unilicensed Band," *Bell Labs Technical Journal*, vol. 2, summer 1997, pp. 118–133.

[28] P. Karn, "MACA - A New Channel Access Method for Packet Radio," in *Proceedings of the 9th ARRL/CRRL Amatuer Radio Computer Networking Conference*, Ontario, Canada, September 1990, pp. 134–140.

[29] R. Kravets and P. Krishnan, "Application-Driven Power Management for Mobile Communication," *ACM/URSI/Baltzer Wireless Networks (WINET)*, vol. 6, no. 4, 1999, pp. 263–277.

[30] M. Krunz, A. Muqattash, and S.-J. Lee, "Transmission Power Control in Wireless

Ad Hoc Networks: Challenges, Solutions, and Open Issues," *IEEE Network*, vol. 18, September/October 2004, pp. 8–14.

[31] P. Lettieri and M. B. Srivastava, "Adaptive Frame Length Control for Improving Wireless Link Throughput, Range, and Energy Efficiency," in *Proceedings of the IEEE International Conference on Computer Communications (INFOCOM)*, San Francisco, CA, vol. 2, March 1998, pp. 564–571.

[32] W. Lewandowski, J. Azoubib, and W. J. Klepczynski, "GPS: Primary Tool for Time Transfer," *Proceedings of the IEEE*, vol. 87, January 1999, pp. 163–172.

[33] J. Li, C. Blake, D. S. J. D. Couto, H. I. Lee, and R. Morris, "Capacity of Ad Hoc Wireless Networks," in *Proceedings of the ACM International Conference on Mobile Computing and Networking (MOBICOM)*, Rome, Italy, July 2001, pp. 61–69.

[34] Q. Li, J. Aslam, and D. Rus, "Online Power-aware Routing in Wireless Ad-hoc Networks," in *Proceedings of the ACM International Conference on Mobile Computing and Networking (MOBICOM)*, Rome, Italy, July 2001, pp. 97–107.

[35] Lucent, *IEEE802.11 WaveLAN PC Card - User's Guide, pp. A-1*. Murray Hill, NJ: Lucent, 1998.

[36] M. J. Miller and N. H. Vaidya, "Improving Power Save Protocols Using Carrier Sensing and Busy-Tones for Dynamic Advertisement Window," University of Illinois at Urbana-Champaign, Tech. Rep., December 2004.

[37] J. P. Monks, V. Bharghavan, and W.-M. Hwu, "A Power Controlled Multiple Access Protocol for Wireless Packet Networks," in *Proceedings of the IEEE International Conference on Computer Communications (INFOCOM)*, Anchorage, AK, April 2001, pp. 219–228.

[38] S. Narayanaswamy, V. Kawadia, R. S. Sreenivas, and P. R. Kumar, "Power Con-

trol in Ad-Hoc Networks: Theory, Architecture, Algorithm and Implementation of the COMPOW protocol," in *Proceedings of the European Wireless*, Florence, Italy, February 2002, pp. 156–162.

[39] N. Poojary, S. V. Krishnamurthy, and S. Dao, "Medium Access Control in a Network of Ad Hoc Mobile Nodes with Heterogeneous Power Capabilities," in *Proceedings of the IEEE International Conference on Communications (ICC)*, Helsinki, Finland, vol. 3, June 2001, pp. 872–877.

[40] M. B. Pursley, H. B. Russell, and J. S. Wysocarski, "Energy-Efficient Transmission and Routing Protocols for Wireless Multiple-hop Networks and Spread-Spectrum Radios," in *EUROCOMM 2000*, Munich, Germany, May 2000, pp. 1–5.

[41] R. Ramanathan and R. Rosales-Hain, "Topology Control of Multihop Wireless Networks using Transmit Power Adjustment," in *Proceedings of the IEEE International Conference on Computer Communications (INFOCOM)*, Tel Aviv, Israel, vol. 2, March 2000, pp. 404–413.

[42] V. Rodoplu and T. H. Meng, "Minimum Energy Mobile Wireless Networks," *IEEE Journal on Selected Areas in Communications*, vol. 17, August 1999, pp. 1333–1344.

[43] M. Sanchez, P. Manzoni, and Z. J. Haas, "Determination of Critical Transmission Range in Ad-Hoc Networks," in *Proceedings of the IEEE Workshop on Multiaccess, Mobility and Teletraffic for Wireless Communications (MMT)*, Venice, Italy, October 1999.

[44] E. Shih, V. Bahl, and M. Sinclair, "Reducing Energy Consumption ofWireless, Mobile Devices Using a Secondary Low-Power Channel," in *MIT Laboratory for Computer Science*, March 2003.

[45] T. Simunic, H. Vikalo, P. Glynn, and G. D. Micheli, "Energy Efficient Design of

Portable Wireless Systems," in *International Symposium on Low Power Electronics and Design (ISLPED)*, Rapallo, Italy, July 2000, pp. 49–54.

[46] S. Singh and C. S. Raghavendra, "PAMAS - Power Aware Multi-Access Protocol with Signalling for Ad Hoc Networks," in *Computer Communications Review*, vol. 28, July 1998, pp. 5–26.

[47] S. Singh, M. Woo, and C. S. Raghavendra, "Power-aware Routing in Mobile Ad Hoc Networks," in *Proceedings of the ACM International Conference on Mobile Computing and Networking (MOBICOM)*, Dallas, TX, October 1998, pp. 181–190.

[48] K. M. Sivalingam, M. B. Srivastava, and P. Agrawal, "Low Power Link and Access Protocols for Wireless Multimedia Networks," in *Proceedings of the Annual Vehicular Technology Conference*, Phoenix, AZ, May 1997, pp. 1331–1335.

[49] M. Stemm and R. H. Katz, "Measuring and Reducing Energy Consumption of Network Interfaces in Hand-Held Devices," *IEICE Transactions on Communications, special Issue on Mobile Computing*, vol. E80-B, no. 8, 1997, pp. 1125–31.

[50] C.-K. Toh, "Maximum Battery Life Routing to Support Ubiquitous Mobile Computing in Wireless Ad Hoc Networks," *IEEE Communications Magazine*, vol. 39, June 2001, pp. 138–147.

[51] Y.-C. Tseng, C.-S. Hsu, and T.-Y. Hsieh, "Power-Saving Protocols for IEEE 802.11-Based Multi-Hop Ad Hoc Networks," in *Proceedings of the IEEE International Conference on Computer Communications (INFOCOM)*, New York, vol. 1, June 2002, pp. 200–209.

[52] R. Wattenhofer, L. Li, P. Bahl, and Y.-M. Wang, "Distributed Topology Control for Power Efficient Operation in Multihop Wireless Ad Hoc Networks," in *Proceedings of the IEEE International Conference on Computer Communications (INFOCOM)*,

Anchorage, AK, vol. 3, April 2001, pp. 1388–1397.

[53] J. E. Wieselthier, G. D. Nguyen, and A. Ephremides, "On the Construction of Energy-Efficient Broadcast and Multicast Trees in Wireless Networks," in *Proceedings of the IEEE International Conference on Computer Communications (INFOCOM)*, Tel Aviv, Israel, March 2000, pp. 585–594.

[54] J. E. Wieselthier, G. D. Nguyen, and A. Ephremides, "Resource-Limited Energy-Efficient Wireless Multicast of Session Traffic," in *Hawaii International Conference on System Sciences HICSS 2001*, Maui, Hawaii, January 2001.

[55] H. Woesner, J.-P. Ebert, M. Schlager, and A. Wolisz, "Power-Saving Mechanisms in Emerging Standards for Wireless LANs: The MAC Level Perspective," *IEEE Personal Communications*, vol. 5, June 1998, pp. 40–48.

[56] S.-L. Wu, Y.-C. Tseng, C.-Y. Lin, and J.-P. Sheu, "A Multi-Channel MAC Protocol with Power Control for Multi-Hop Mobile Ad Hoc Networks," *The Computer Journal (SCI)*, vol. 45, no. 1, 2002, pp. 101–110.

[57] S.-L. Wu, Y.-C. Tseng, and J.-P. Sheu, "Intelligent Medium Access for Mobile Ad Hoc Networks with Busy Tones and Power Control," *IEEE Journal on Selected Areas in Communications*, vol. 18, September 2000, pp. 1647–1657.

[58] Y. Xu, J. Heidemann, and D. Estrin, "Geography-informed Energy Conservation for Ad Hoc Routing," in *Proceedings of the ACM International Conference on Mobile Computing and Networking (MOBICOM)*, Rome, Italy, July 2001, pp. 70–84.

[59] W. Ye, J. Heidemann, and D. Estrin, "An Energy-Efficient MAC Protocol for Wireless Sensor Networks," in *Proceedings of the IEEE International Conference on Computer Communications (INFOCOM)*, New York, June 2002, pp. 1567–1576.

[60] R. Zheng and R. Kravets, "On-demand Power Management for Ad Hoc Network,"

in *Proceedings of the IEEE International Conference on Computer Communications (INFOCOM)*, San Franciso, CA, vol. 1, April 2003, pp. 481–491.

[61] H. Zhu, G. Cao, G. Kesidis, and C. Das, "An Adaptive Power-Conserving Service Discipline for Bluetooth," in *Proceedings of the IEEE International Conference on Communications (ICC)*, New York, vol. 1, April 2002, pp. 303–307.

[62] M. Zorzi and R. R. Rao, "Is TCP energy efficient?," in *Proceedings of the IEEE International Workshop on Mobile Multimedia Communications (MoMuC)*, San Diego, CA, November 1999, pp. 198–201.

VITA

Eun-Sun Jung received a B.S. degree in Computer Science and Statistics from Dankook University, Korea, in 1995, and an M.S. degree in Information Security from University of London, U.K., in 1998. From 1995 to 1996 she was a member of technical staff in Hanwha Corporation, Korea. In 1999, she was employed by Korea Information Security Agency as a research scientist. Her research interests include mobile computing and wireless networks. She can be reached at esjung@cs.tamu.edu.